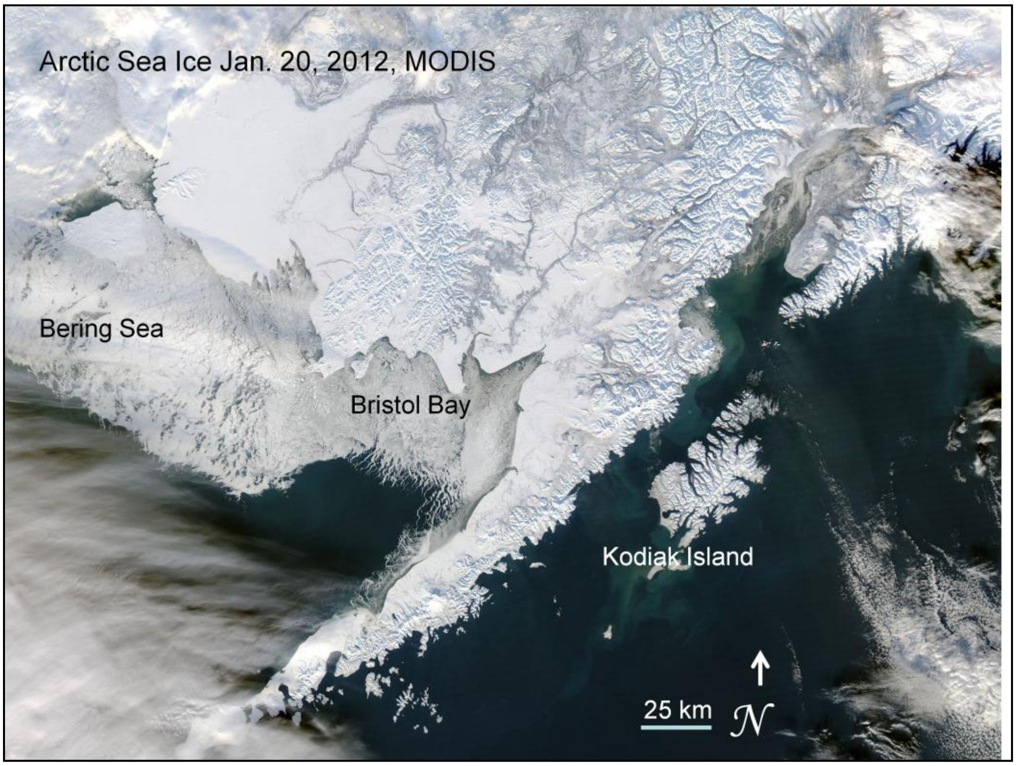

Snow rested on the land surface while ice rested on the sea surface in southwestern Alaska in mid-January 2012. The Moderate Resolution Imaging Spectroradiometer (MODIS) on NASA's Aqua satellite captured this natural-color image on January 15. Pristine snow blankets the mountains and plains, and tendrils of sea ice fill Bristol Bay.

Arctic sea ice waxes and wanes throughout the year, and conditions fluctuate each season and year—including conditions in the Bering Sea. Although sea ice extent in mid-January 2012 was not at a record high, it was the highest ice extent in several years, according to the National Snow and Ice Data Center.

North of the area in this image, in Nome, Alaska, harsh weather conditions hampered the delivery of much-needed winter fuel. A strong storm in November 2011 prevented the customary pre-winter fuel delivery, and thick sea ice hampered efforts to reach the area through mid-January. A Russian tanker finally succeeded in delivering fuel to Nome by January 16, 2012.

Overall, Arctic sea ice typically grows throughout the month of January, reaching its peak in late February or March. For animations of Arctic sea ice minimum and maximum extents, see the World of Change feature onArctic sea ice.

References

Associated Press. (2012, January 16). Nome, Alaska, finally gets Russian tanker fuel. CBS News. Accessed January 20, 2012.

National Snow and Ice Data Center (n.d.) Multisensor Analyzed Sea Ice Extent—

Northern Hemisphere Browse Regions and Bering Sea. Accessed January 20, 2012.

NASA images courtesy Jeff Schmaltz, LANCE/EOSDIS MODIS Rapid Response Team at NASA GSFC. Caption by Michon Scott.

Instrument: Aqua - MODIS

Russian icebreaker “Renda” and USCS Cutter Healy. The US ship could not enter the harbor. Last week they delivered 1.3 M gal. fuel to Nome, AK.

The Spectroscopy of Water

Lecture 5 January 24, 2012 Water

Chapter 12, 8, 9

Spectral properties of phases of water (vapor, liquid, solid)

Land Processes: The Medium Resolution Earth Observing Satellites

Landsat series: Multispectral Scanner (MSS) and Thematic Mapper (TM)

SPOT series

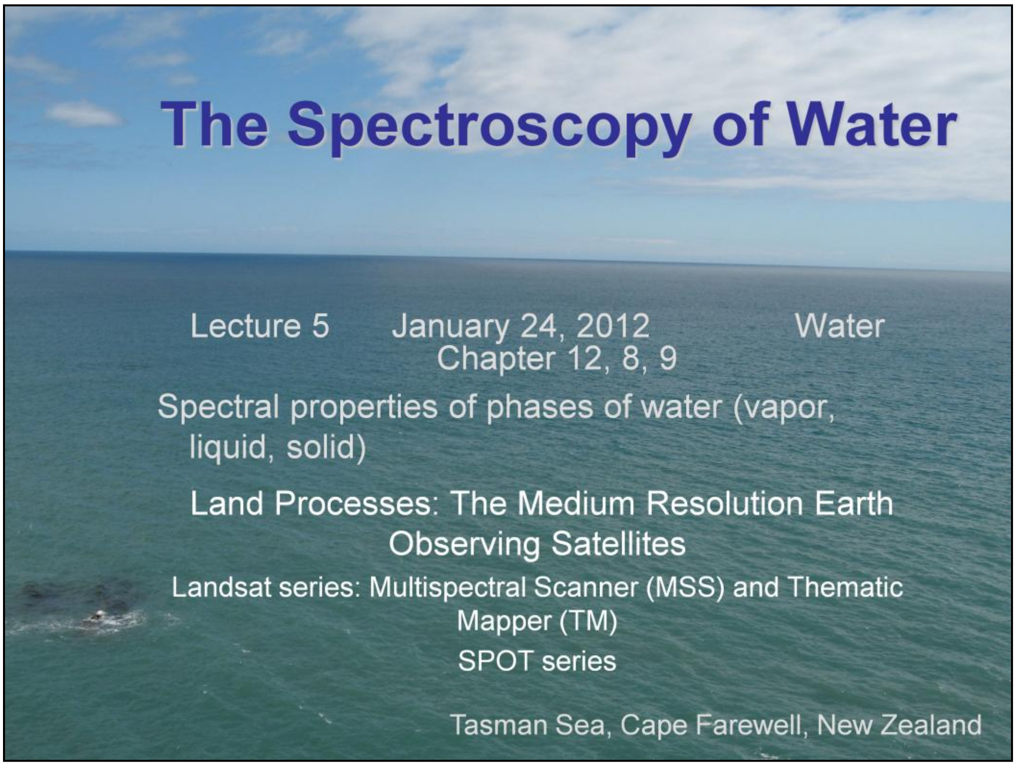

Tasman Sea, Cape Farewell, New Zealand

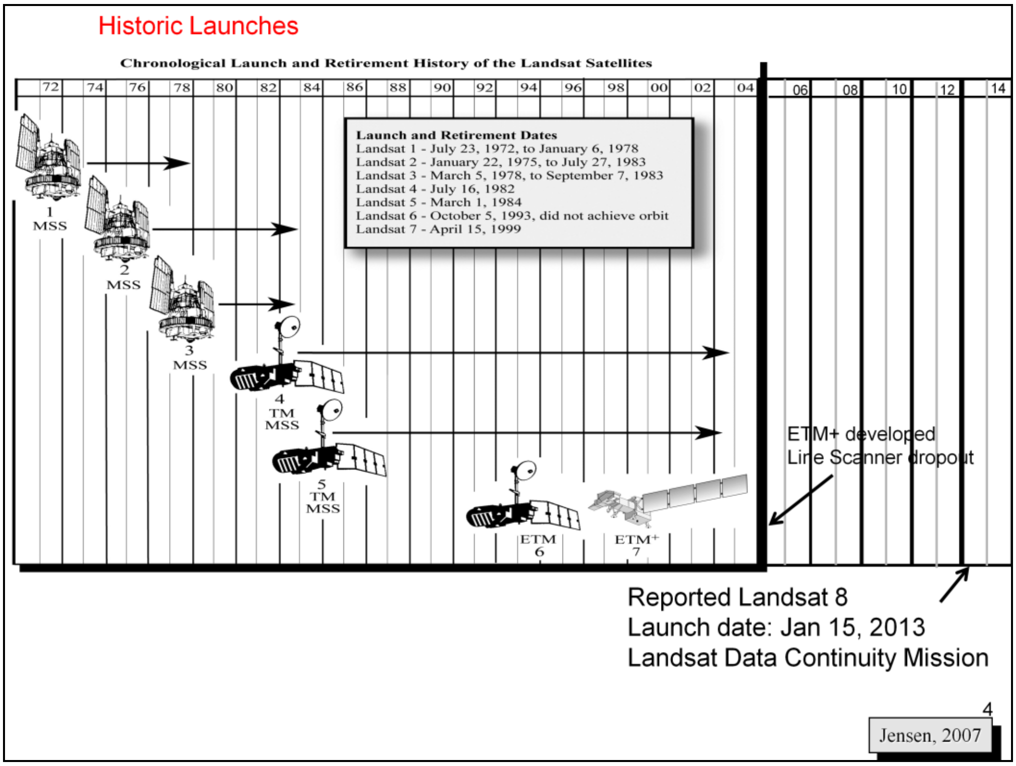

Notice that first three look alike and then next three are similar, than #7 changes again. What does this suggest about the instruments on these platforms?

http://www.itc.nl/research/products/sensordb/Launch_Schedule.aspx

Faculty of Geo-Information Science and Earth Observation of the University of Twente

Home | Search | Sitemap | Contact us

Research

About ITC Research Education Project Services Alumni Partnerships News

Launch schedule

For information on Satellites and Sensors : ITC's database of Satellites and Sensors

1999 2000 2001 2002 2003 2004 2005 2006 2007 2008 2009 2010 2011 2012 2013 2014 2015 2016 2017 2018 2019

Sensor/Platform	Information from	(Scheduled) launch date
	1999	
FORMOSAT-1 (ROCSAT-1)	National Space Program Office	Launched 27 January
SunSat	SUNSAT Homepage	Launched 26 February
INSAT 2E	ISRO	Launched 2 April
Landsat 7	Landsat 7 Home Page	Launched 15 April
UoSat-12	SSTL	Launched 21 April
Ikonos-1	Space Imaging	**Failed** 27 April
Fengyun-1C	National Satellite Meteorological Center, China	Launched 10 May
IRS-P4 (Oceansat)	ISRO	Launched 26 May
KitSat-3 (Wooribyul-3)	SaTReC	Launched 26 May
DLR-Tubsat	DLR-TUBSAT	Launched 26 May
QuikSCAT	SeaWinds on QuikSCAT	Launched 20 June
Okean-O#1	Sputnik Home page	Launched 17 July
Ikonos	Space Imaging	Launched 24 September
RESURS-F1M#2 (22)	EU and Russia in Space	Launched 28 September
CBERS 1	INPE-CBERS	Launched 14 October
MTSat	MTSAT	**Failed** 15 November
Helios 1B		Launched 3 December

Landsat I (ERTS 1):Multispectral Scanner(MSS)

Polar, Sun-synchronous Orbit

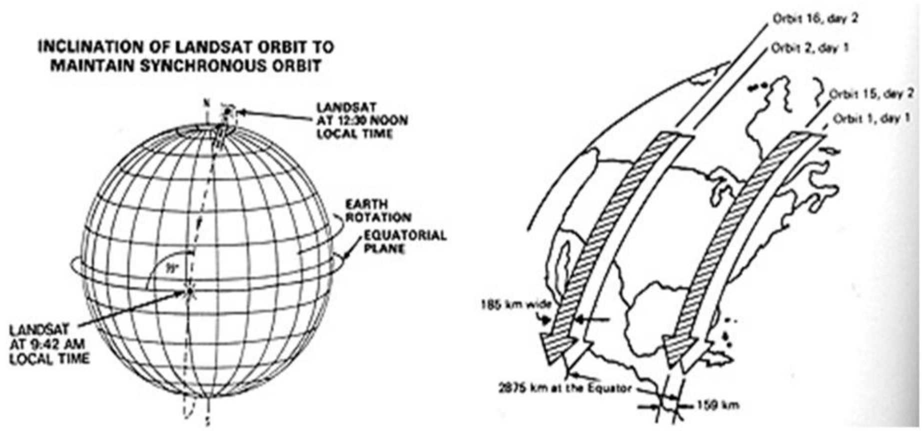

Near Polar, Sun Synchronous, Morning overpass between 9:30-10am
14 passes/day with 103 min. orbit; ~80m pixels swath is 185 km wide

6

The first one to three Landsats orbited at an altitude of 570 miles (923 km);
4 and 5 at 435 miles (705 km).

The orbits of all Landsats are near-polar (inclined 9.09° from a longitudinal line) and Sun-synchronous (pass every time over the equator between 9:30 and 10:00 AM), making 14 passes in descending mode (southward from the North pole in the daylight mode) each day (about 103 minutes for a complete orbital circuit). After any given orbit, the spacecraft will occupy its next orbit some 1775 miles (2875 km) to the west; on the next day, the orbits are so configured so that orbit 15 has displaced westward by 98 miles (159 km) at the equator.

Landsats 1-3 will reoccupy almost precisely the same orbit after 252 such orbits, or 18 days later; Landsats 4 and 5 reoccupy on a 16 day cycle. Under the above orbital conditions, and with an angular field of view if 11.58 ° the width of a Landsat MSS scene is 185 km (114 statute or 100 nautical miles). The continuing orbital strip is cut every 185 km to produce a given image' length. These same frame dimensions hold for the Landsat Thematic Mapper (TM) images.

1 scene: 185 mi x 185 mi = 13,300 sq. miles; 33,225 sq. km; 8,512,000 acres

Orbit Tracks of Landsat 1, 2, or 3 During A Single Day of Coverage

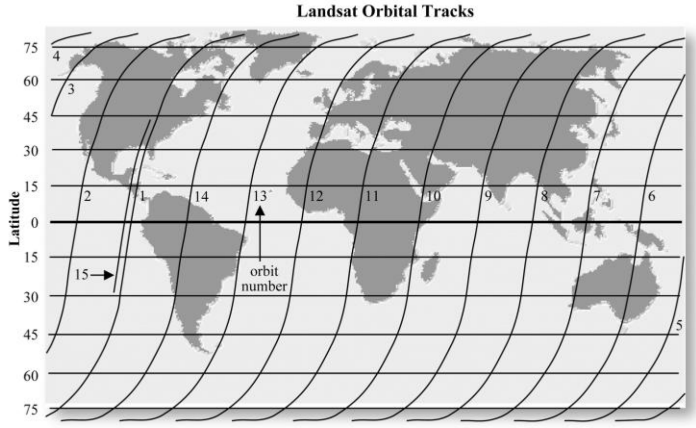

Jensen, 2007

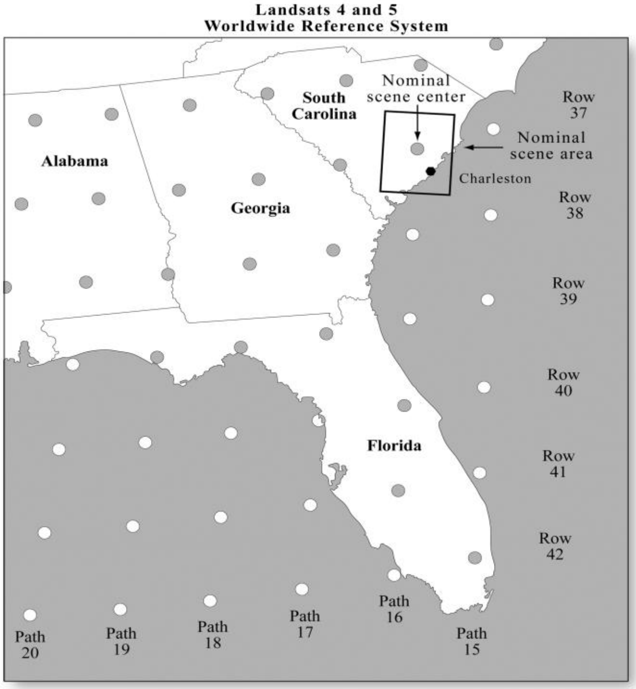

Landsat “scenes” are provided in blocks of 185 km x 185km;

New mode (as of 2009) will let you specify area to be downloaded using

8

Jensen, 2007

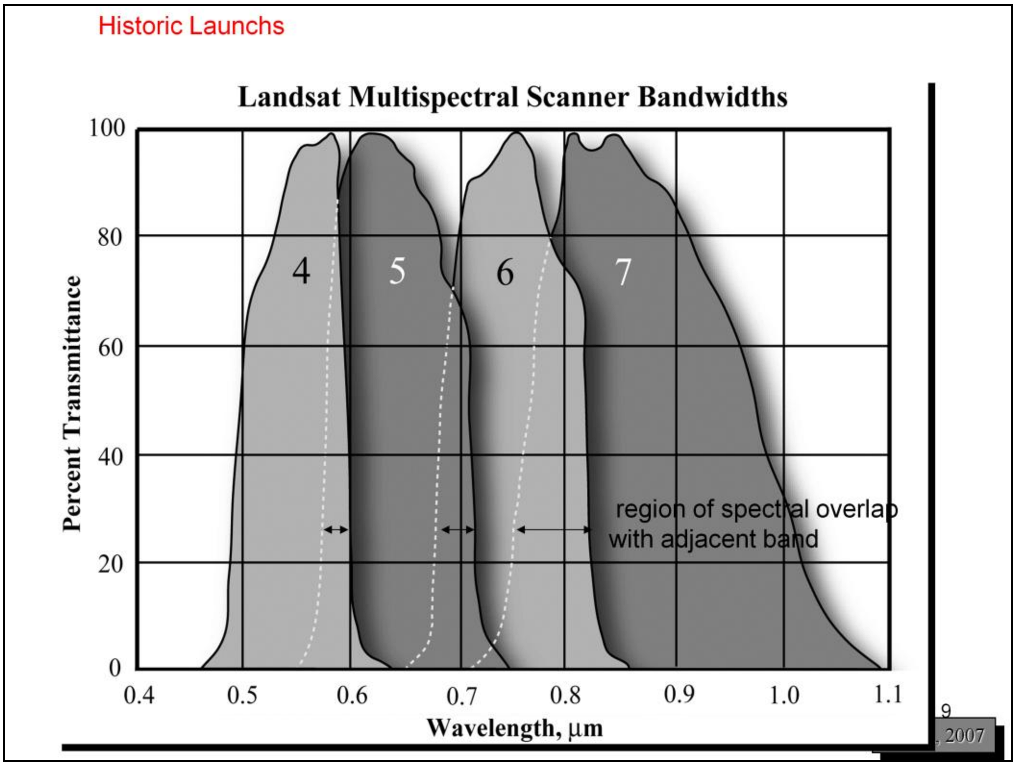

Due to issues with the detector sensitivity and the filters used in fabricating the detector, band passes do not have non-overlapping square-wave structure but are sensitive to some wavelengths more than others and some wavelengths are detected by more than one band.

Newer instruments have less overlap and more Gaussian-shaped sensitivities.

Why are bands called band 4, 5, 6, 7? This is an artifact of how the instruments were designed and earlier bands (not used on MSS) were termed bands 1, 2, 3.

Historic Launchs

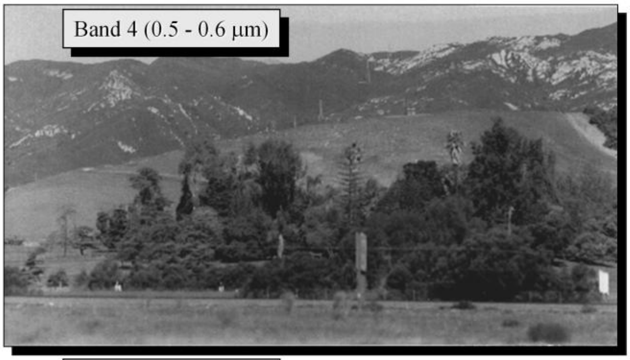

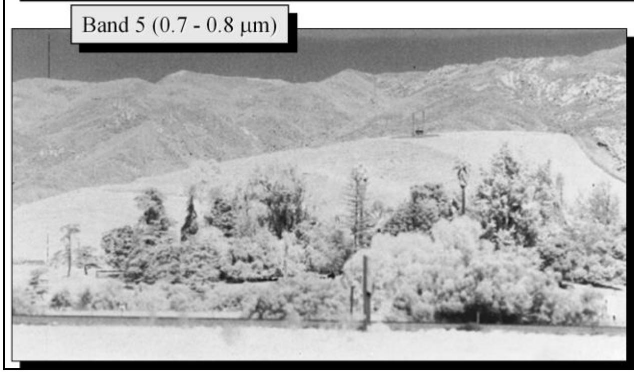

Landsat MSS
Terrestrial Images of Goleta, CA Obtained on March 4, 1972

Jensen, 2007

Landsat 5 Flight Segment

27 years of on-orbit operations

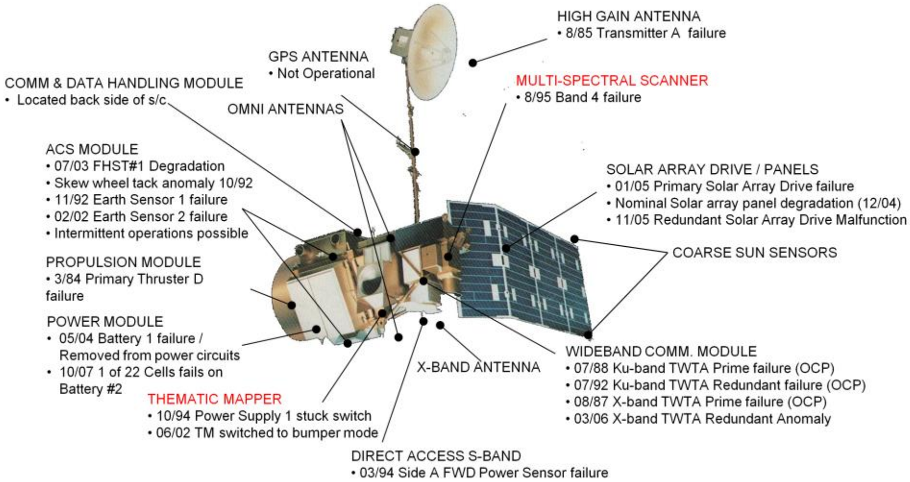

Landsat Multispectral Scanner (MSS) and Landsat Thematic Mapper (TM) Sensor System Characteristics

	Landsat Multispectral Scanner (MSS)			Landsat 4 and 5 Thematic Mapper (TM)		
	Band	Spectral Resolution (μm)	Radiometric Sensitivity (NEΔP)[a]	Band	Spectral Resolution (μm)	Radiometric Sensitivity (NEΔP)
	4[b]	0.5 – 0.6	0.57	1	0.45 – 0.52	0.8
	5	0.6 – 0.7	0.57	2	0.52 – 0.60	0.5
	6	0.7 – 0.8	0.65	3	0.63 – 0.69	0.5
	7	0.8 – 1.1	0.70	4	0.76 – 0.90	0.5
	8[c]	10.4 – 12.6	1.4K (NEΔT)	5	1.55 – 1.75	1.0
				6	10.40–12.5	0.5 (NEΔT)
				7	2.08–2.35	2.4
IFOV at nadir	79 × 79 m for bands 4 through 7 240 × 240 m for band 8			30 × 30 m for bands 1 through 5, 7 120 × 120 m for band 6		
Data rate	15 Mb/s			85 Mb/s		
Quantization levels	6 bit (values from 0 to 63)			8 bit (values from 0 to 255)		
Earth coverage	18 days Landsat 1, 2, 3 16 days Landsat 4, 5			16 days Landsat 4, 5		
Altitude	919 km			705 km		
Swath width	185 km			185 km		
Inclination	99°			98.2°		

[a] The radiometric sensitivities are the noise-equivalent reflectance differences for the reflective channels expressed as percentages (NEΔP) and temperature differences for the thermal infrared bands (NEΔT).
[b] MSS bands 4, 5, 6, and 7 were renumbered bands 1, 2, 3, and 4 on Landsats 4 and 5.
[c] MSS band 8 was present only on Landsat 3.

Jensen, 2007

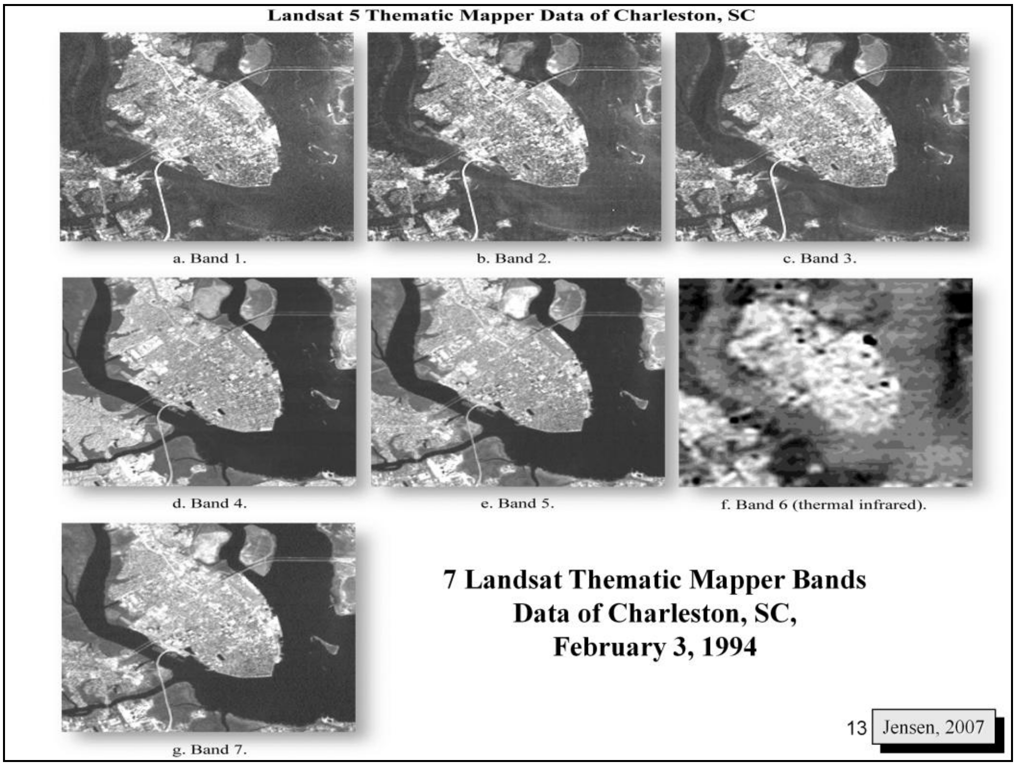

Note: In Landsat TM use, the thermal infrared band is band 6 and the SWIR band is band 7.

Landsat 7 Flight Segment

~12 years of on-orbit operations

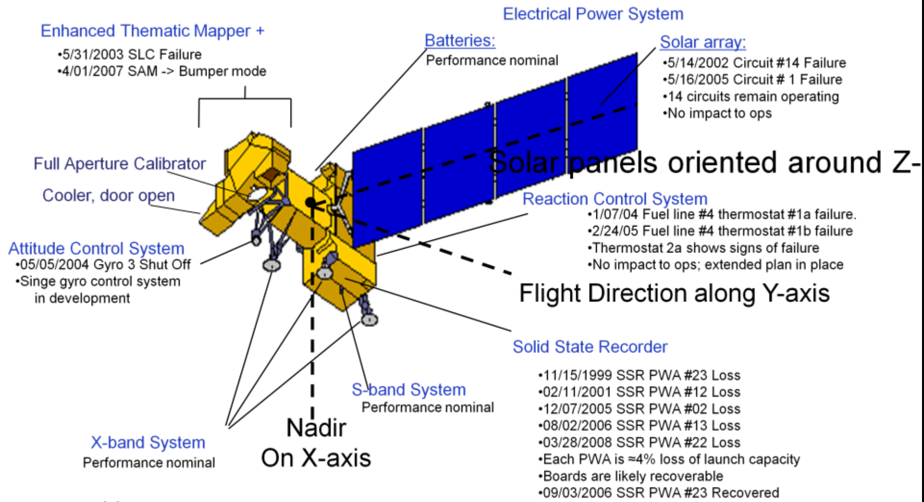

16 day repeat orbits
9:30-10am overpass
30m pixels
(185 X 185) km^2 swaths

TM 5 and Landsat 7 - ETM+ Spectral Bandwidths								
Bandwidth (µ) Full Width - Half Maximum								
Sensor	**Band 1**	**Band 2**	**Band 3**	**Band 4**	**Band 5**	**Band 6**	**Band 7**	**Band 8**
TM	0.45 - 0.52	0.52 - 0.60	0.63 - 0.69	0.76 - 0.90	1.55 - 1.75	10.4 - 12.5	2.08 - 2.35	N/A
ETM+	0.45 - 0.52	0.53 - 0.61	0.63 - 0.69	0.78 - 0.90	1.55 - 1.75	10.4 - 12.5	2.09 - 2.35	.52 - .90

Bandwidth Described as the Full bandwidth at half-maximum Intensity (FWHM)

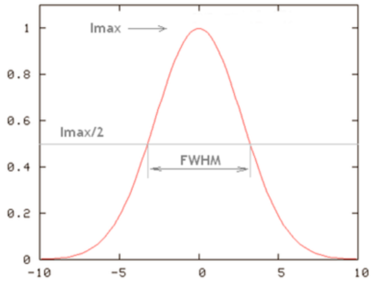

15

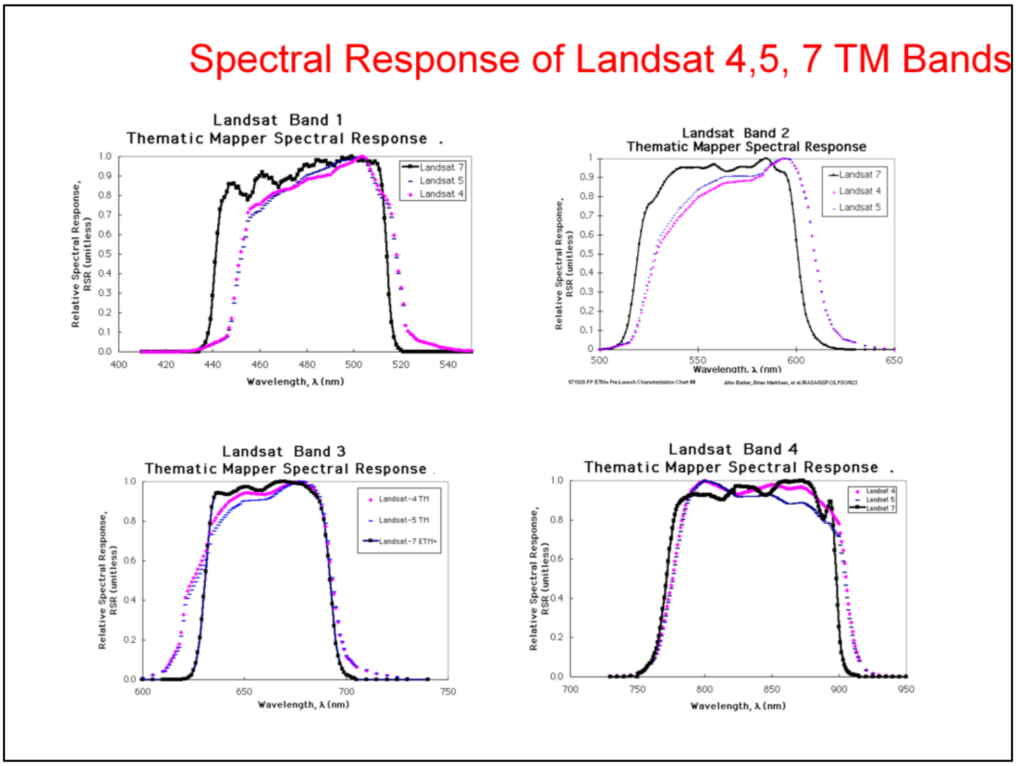

As the instruments in a series evolve with different versions, the data recorded also changes. This example shows spectrometer differences for recent Landsat TM series 4, 5, 7. Differences between different instruments are significantly greater than this. Thus when someone produces an NDVI or EVI or some other index with different instruments, the differences between instruments may be greater than the actual spectral differences.

Spectral Response of Landsat 4, 5, 7 TM Bands

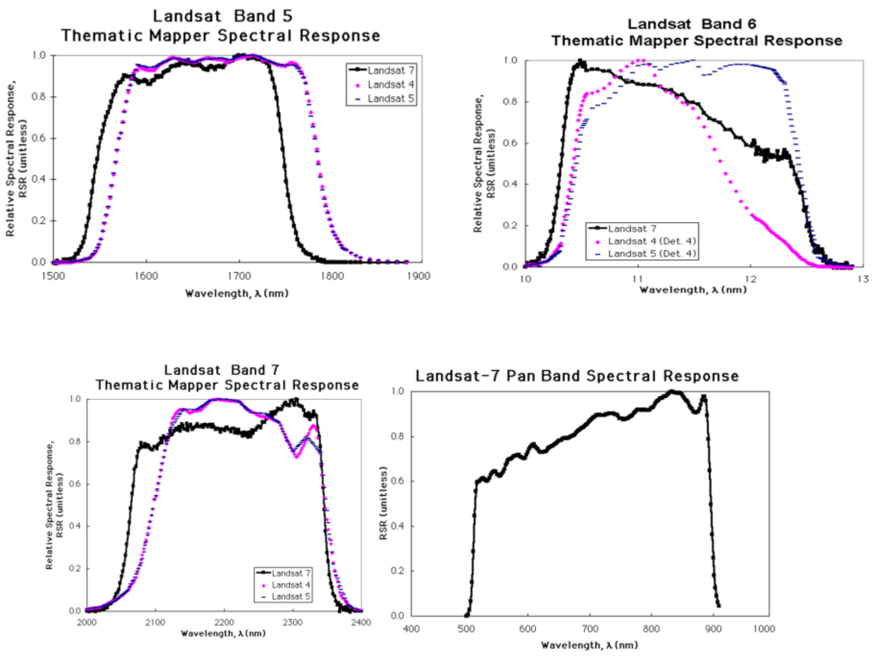

March 30, 1975 MSS view of central San Diego. California at 80m resolution CIR.

330 × 282 pixels. It shows the Bay harbors, military and civilian airports, the downtown, Balboa Park, Mission Bay, and Cabrillo Point.

Landsat 7 Enhanced Thematic Mapper Plus Imagery of San Diego, CA

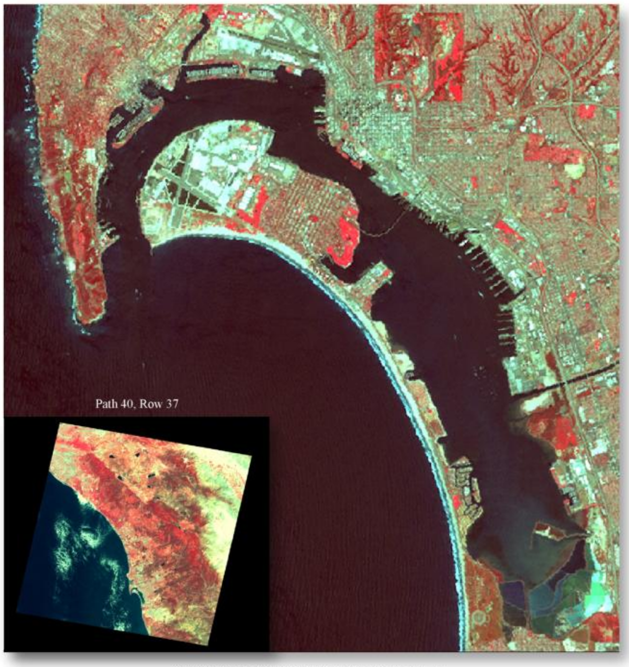

Color-infrared color composite (RGB = bands 4, 3, 2).

Landsat 7
ETM^+

19

What bands are these?

November 22, 1988, SPOT image of San Diego, 3multispectral HRV bands at 20 m resolution, are combined and registered with the 10 m panchromatic image

SPOT (Satellite Pour l'Observation de la Terre)

Satellites	SPOT 1	(21/02/1986 - 1990
	SPOT 2	(21/01/1990 - 2009
	SPOT 3	(25/09/1993 - 14/11/1997)

altitude: 832 km
inclination: 98 degrees
orbit: sun-synchronous polar
period of revolution: 101 minutes; 14 + 5/26 orbits per day
repeat cycle: 26 day (2 and 3 were phased 13 days apart)

Mode	Band	Spectral band	Resolution
XS-multispectral	XS1	0.50 – 0.59 µm	20m x 20m
	XS2	0.61 – 0.68 µm	20m x 20m
	XS3	0.79 – 0.89 µm	20m x 20m
P-panchromatic	PAN	0.51 – 0.73 µm	10m x 10m

21

The SPOT (Satellites Pour l’Observation de la Terre or Earth-observing Satellites) remote-sensing program was set up by France in partnership with Belgium and Sweden. The constellation of SPOT satellites in orbit makes it possible to observe practically the entire planet in one day. Above 40° N. and S. latitude any point whatsoever can be observed each day of the year, whereas at the Equator itself a thin, approximately 250km-wide strip (out of the 2,800 km separating the two adjacent SPOT satellite orbits) remains inaccessible on any given day. Two stereoscopic scenes can be acquired in tandem mode on the same day by using two of the three satellites in the course of a 26-day cycle.

HRV sensors
Each HRV sensor can acquire the images in panchromatic mode (P mode: a single wide band in the visible part of the spectrum) or multispectral mode (XS mode: the green, red, and infrared bands of the electromagnetic spectrum) indifferently. The two HRV sensors can function independently or in tandem in either XS or P mode. Each of the two HRV instruments can sweep a 60km-wide swath. They thus acquire 60km x 60km images. The images’ spatial resolution is 10m x 10m for the panchromatic images and 20m x 20m for the multispectral images

SPOT 4

Two identical HRVIR (Visible & Infrared High-Resolution) optical sensors and the VEGETATION sensor,

altitude: 830 km
inclination: 98 degrees
orbit: sun-synchronous polar
period of revolution: 101 minutes
repeat cycle: 26 days; constellation + pointing allows 2-3 day repeat
satellite: SPOT 4 (24/03/1998 – still operational)

New middle-infrared band (1.58-1.75 µm);

Old panchromatic band (0.51-0.73 µm) band replaced by the B2 (0.61-0.68 µm) band, which functions equally well in ‘10m’ and ‘20m’ mode; and onboard superimposition of all of the spectral bands.

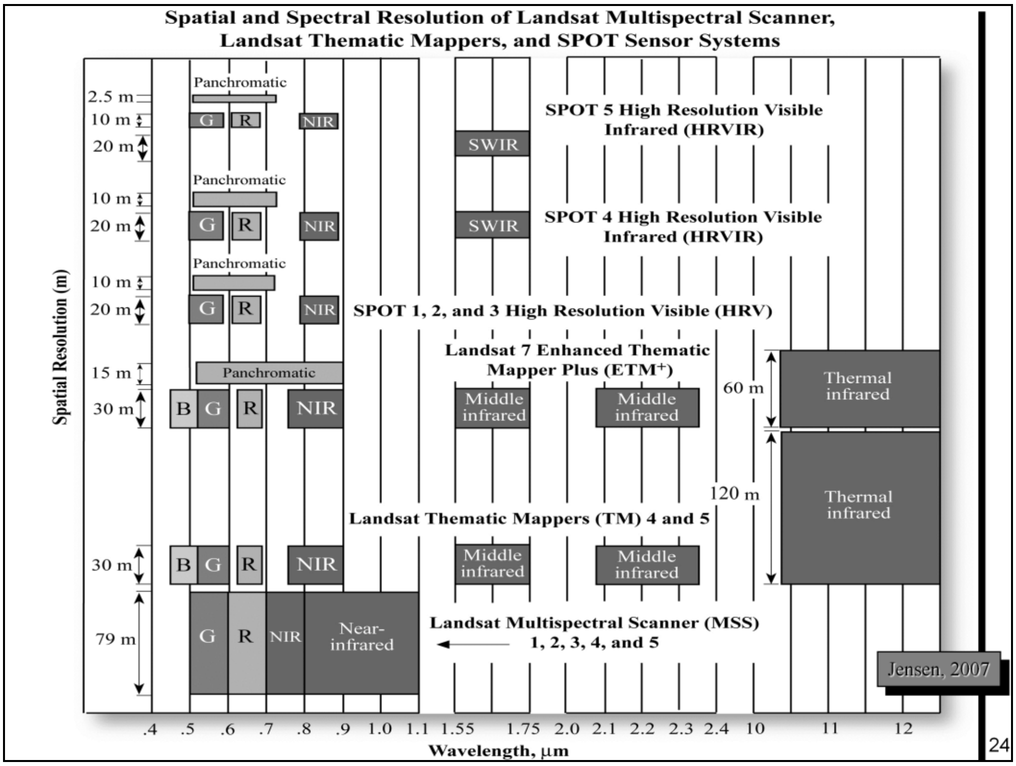

Spatial and Spectral Resolution of Landsat Multispectral Scanner, Landsat Thematic Mappers, and SPOT Sensor Systems
Spatial Resolution (m)
Wavelength, μm
SPOT 5 High Resolution Visible Infrared (HRVIR)
SPOT 4 High Resolution Visible Infrared (HRVIR)
SPOT 1, 2, and 3 High Resolution Visible (HRV)
Landsat 7 Enhanced Thematic Mapper Plus (ETM+)
Landsat Thematic Mappers (TM) 4 and 5
Landsat Multispectral Scanner (MSS) 1, 2, 3, 4, and 5
Panchromatic
SWIR
Middle infrared
Thermal infrared
Near-infrared
NIR
2.5 m
10 m
15 m
20 m
30 m
60 m
79 m
120 m
Jensen, 2007
24

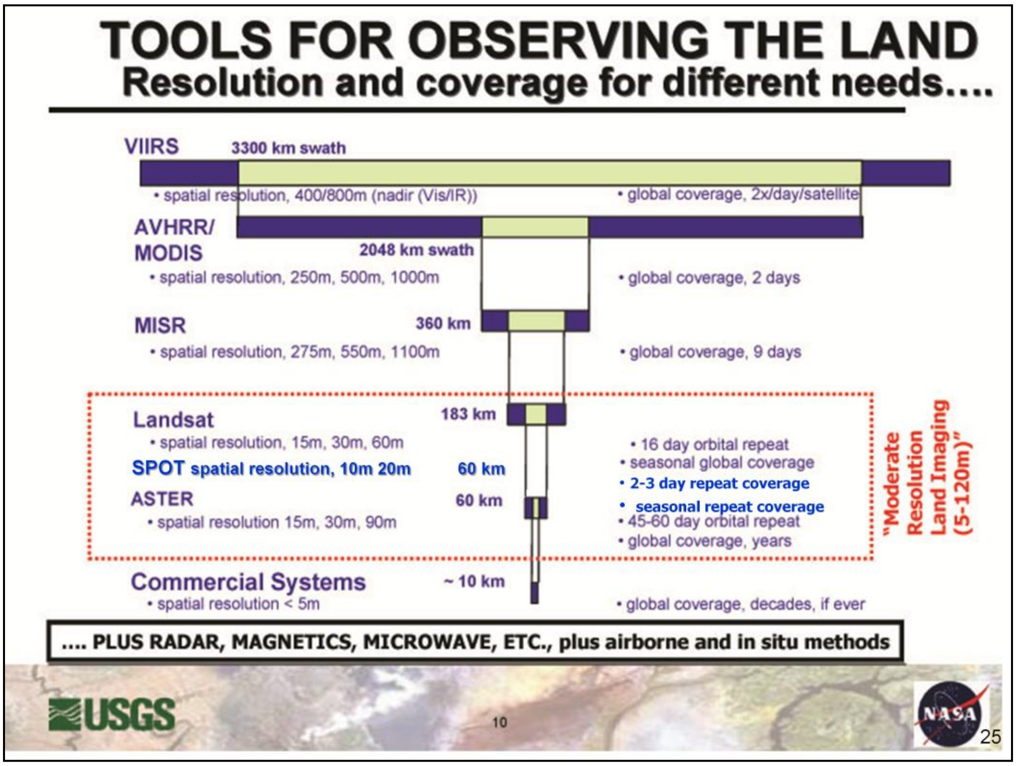
TOOLS FOR OBSERVING THE LAND
Resolution and coverage for different needs….
VIIRS
3300 km swath
• spatial resolution, 400/800m (nadir (Vis/IR))
• global coverage, 2x/day/satellite
AVHRR/ MODIS
2048 km swath
• spatial resolution, 250m, 500m, 1000m
• global coverage, 2 days
MISR
360 km
• spatial resolution, 275m, 550m, 1100m
• global coverage, 9 days
Landsat
183 km
• spatial resolution, 15m, 30m, 60m
• 16 day orbital repeat
• seasonal global coverage
SPOT spatial resolution, 10m 20m
60 km
• 2-3 day repeat coverage
• seasonal repeat coverage
ASTER
60 km
• spatial resolution 15m, 30m, 90m
• 45-60 day orbital repeat
• global coverage, years
"Moderate Resolution Land Imaging (5-120m)"
Commercial Systems
~ 10 km
• spatial resolution < 5m
• global coverage, decades, if ever
…. PLUS RADAR, MAGNETICS, MICROWAVE, ETC., plus airborne and in situ methods
USGS
10
NASA
25

Landsat Synoptic Coverage

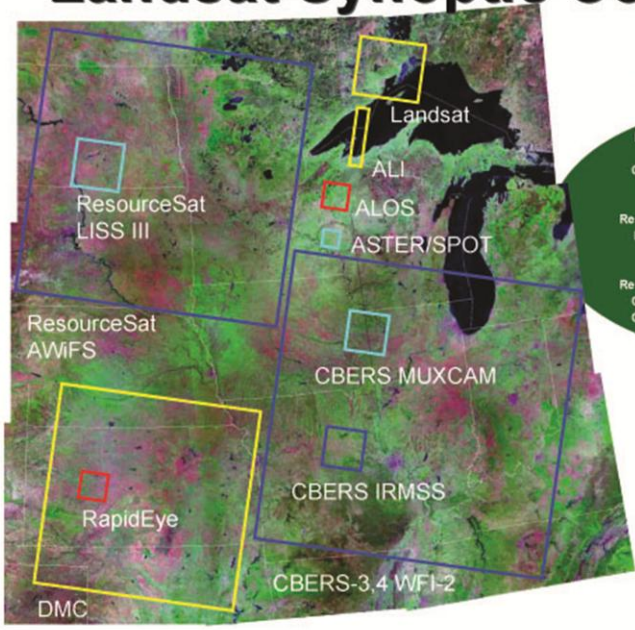

Satellite	Sensor	Ground Sample Distance (m)
RapidEye	REIS	6.5
ALOS	AVNIR	10
CBERS-3,4	MUXCAM	20
SPOT 5	HRG	10/20
Terra	ASTER	15/30/90
ResourceSat-1	LISS III+	23.5
Landsat 7	ETM+	15/30/60
EO-1	ALI	30
DMC	MSDMC	32
ResourceSat-1	AWiFS*	[illegible]
CBERS-3,4	WFI-2	[illegible]
CBERS-3,4	IRMSS	[illegible]

Note: For purposes of scene size comparison only. Locations do not represent actual orbital paths or operational acquisitions.

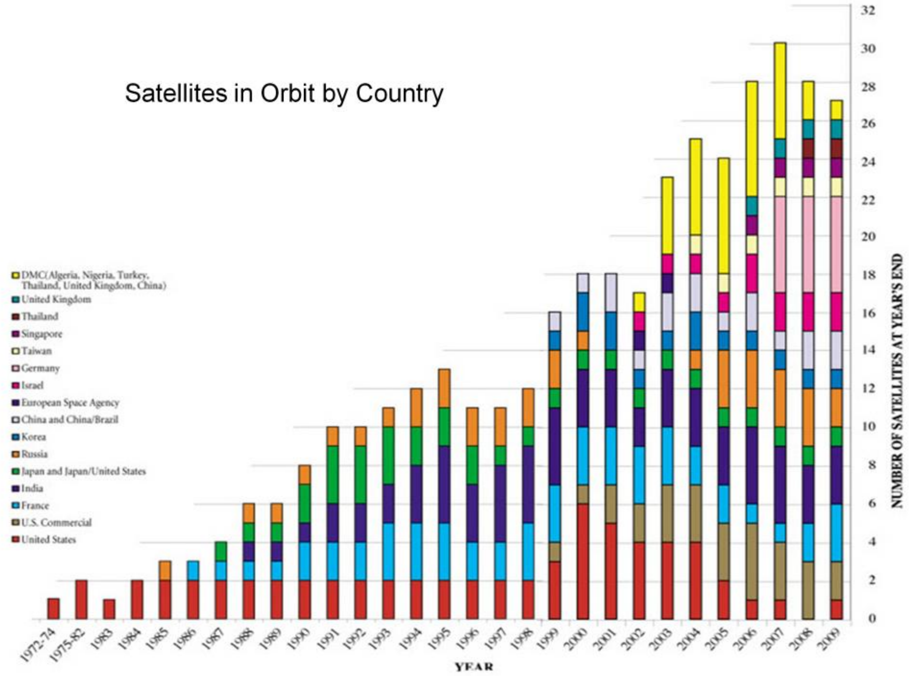

Figure 1. Significant multispectral sensor technology advances were made between the time Landsat 1 launched in 1972 and Landsat 4 launched in 1982. The period from 1978 to 1998 was dominated by the entry of the foreign systems. Now there are 25 satellites in orbit—double the number in 1998—and five more are expected to launch by 2007. Plus a lot more countries are paying for them.

Absorption of energy by water

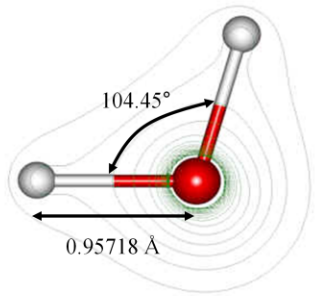

water molecule has 3 degrees of vibrational freedom

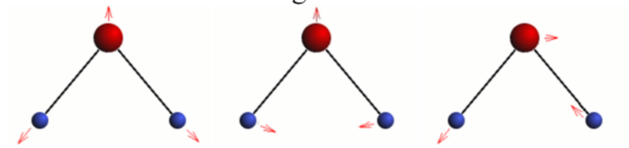

Symmetric stretching mode at $v1$ = 2.73 µm

Bending mode at $v2$ = 6.27 µm

Asymmetric stretching mode at $v3$ = 2.66 µm

Combination	Liquid state
$v1+v3$	0.739 µm
$2v1+v3$	0.970 µm
$v1+v2+v3$	1.200 µm
$v1+v3$	1.450 µm
$v2+v3$	1.940 µm

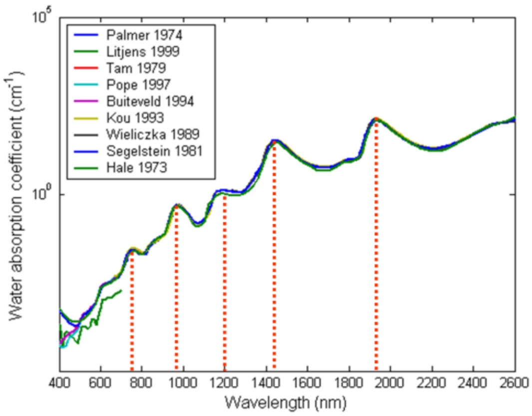

http://omlc.ogi.edu/spectra/water/

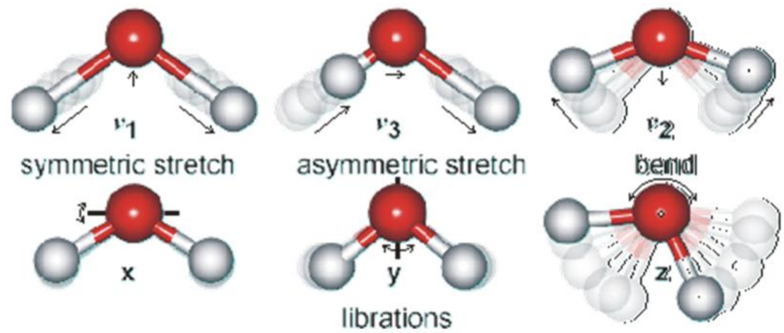

Librations: a real or apparent oscillatory motion

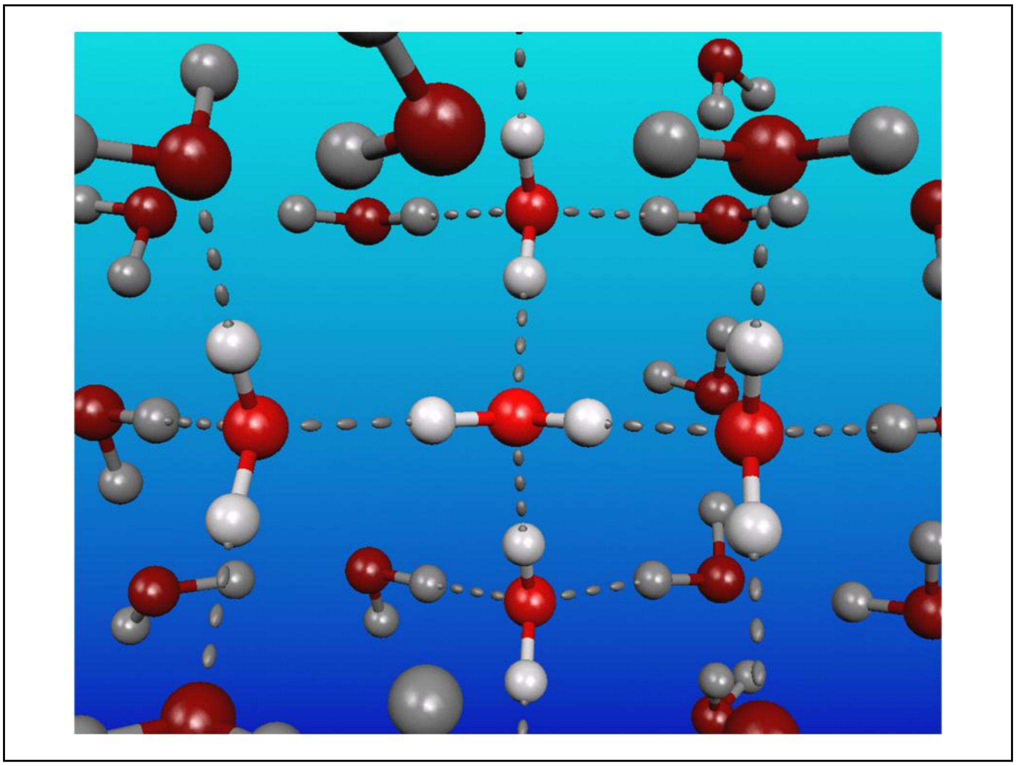

The hydrogen bonding network of neat liquid water (H_2O) shows rearrangements and energy redistribution on time scales much faster than any other liquid, underlining its particular role in Nature.

A team of researchers at the Max Born Institut in Berlin and the University of Toronto have solved the long standing problem whether for liquid water O-H stretching vibrational line shapes are determined by slowly varying hydrogen bond networks or by rapidly fluctuating and interchanging configurations.

Stretching vibration of the water molecule. An ultrashort infrared pulse excites the asymmetric stretching vibration of the angled water molecule (red: oxygen atom, gray: hydrogen atom). The water molecule is part of a network of hydrogen bonds between the hydrogen and oxygen atoms on neighboring molecules (small gray symbols). Shown are the elongations of the atoms during the stretching vibration with a vibrational period of 10 fs. (Animation by Jens Dreyer, MBI)

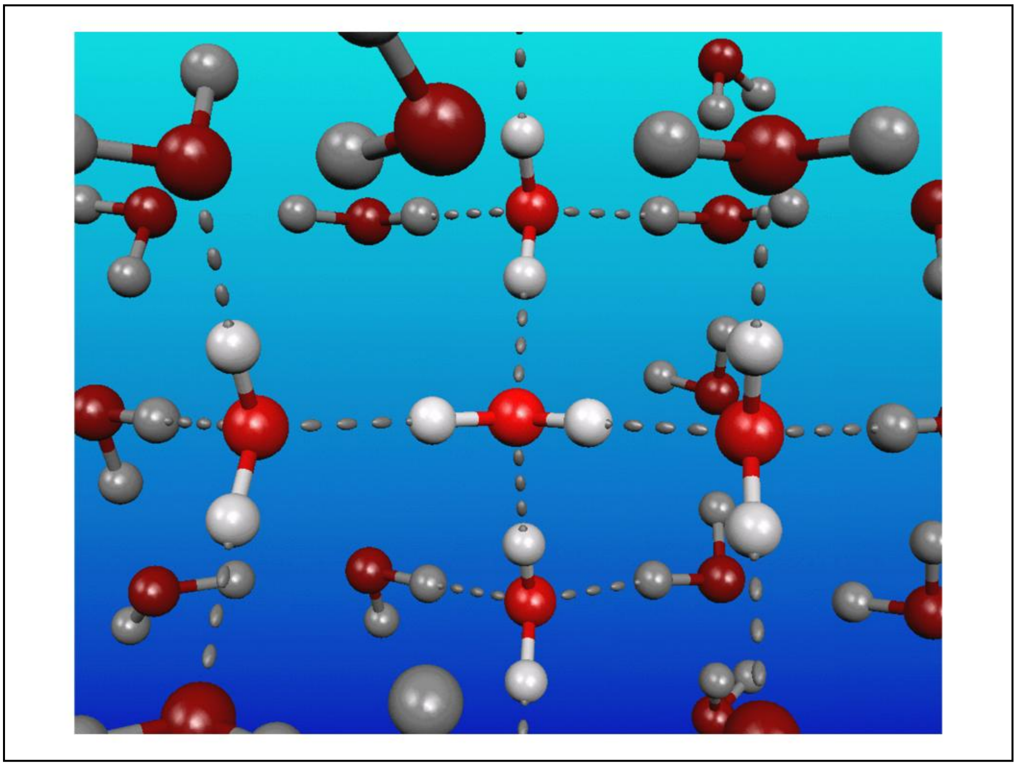

Librational motion of water. Librational motions change the relative orientation of water molecules and - thus - contribute to the loss of structural memory in the liquid. A period of the librational mode shown lasts approximately 40 fs. (Animation by Jens Dreyer, MBI)

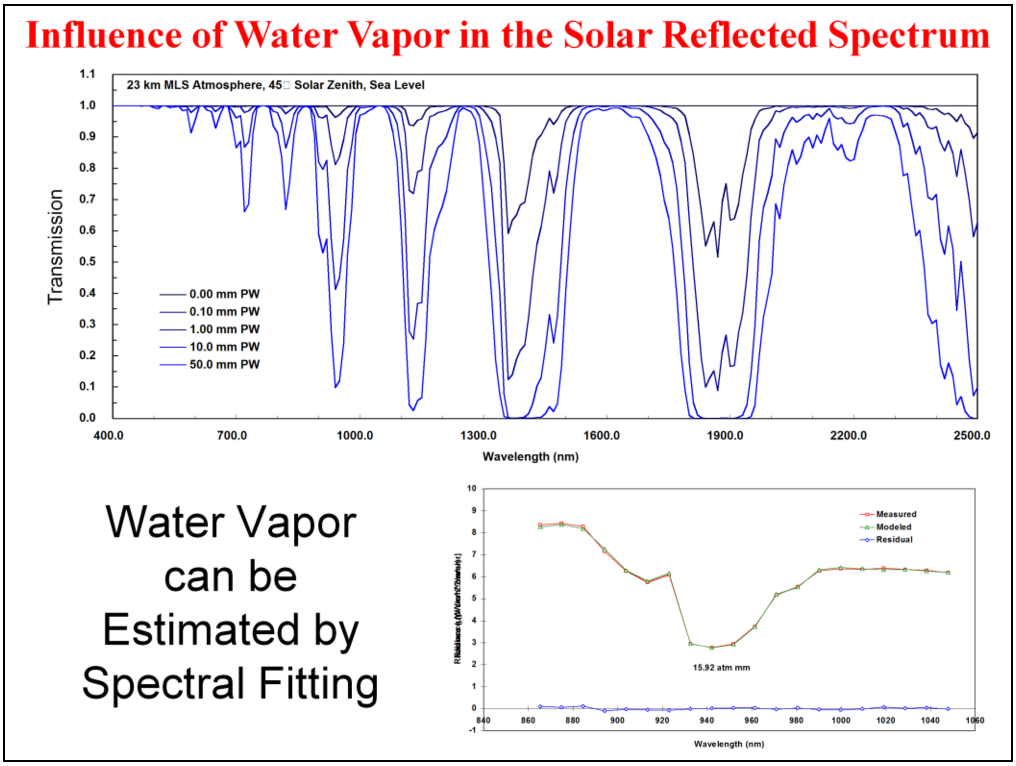

Note that the absorption features become deeper and broader (more wavelengths involved) as water vapor in the atmosphere increases.

Reflectance of Clouds…

— *increases* with *decreasing* droplet size - why?

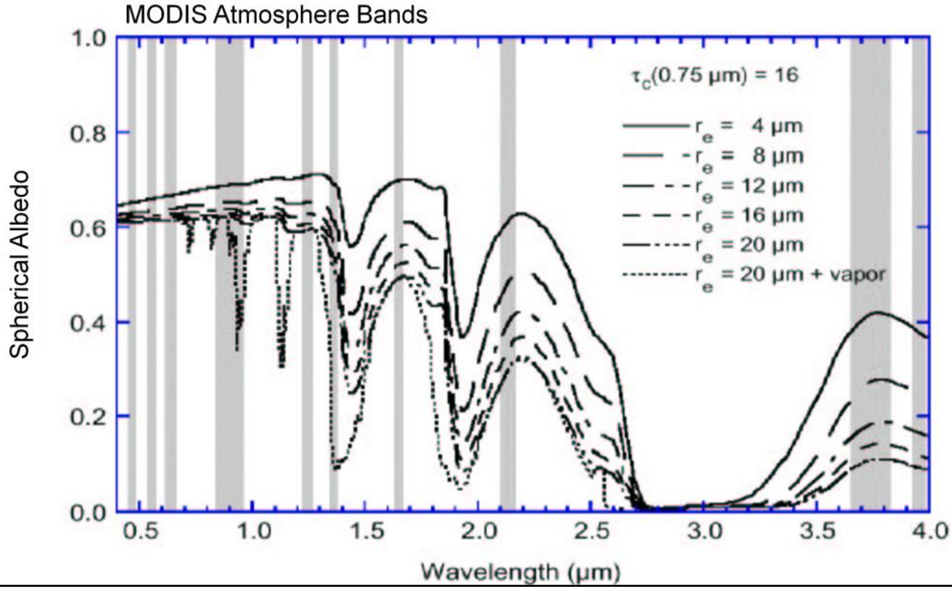

AVIRIS Water Vapor at Rogers Dry Lake, CA

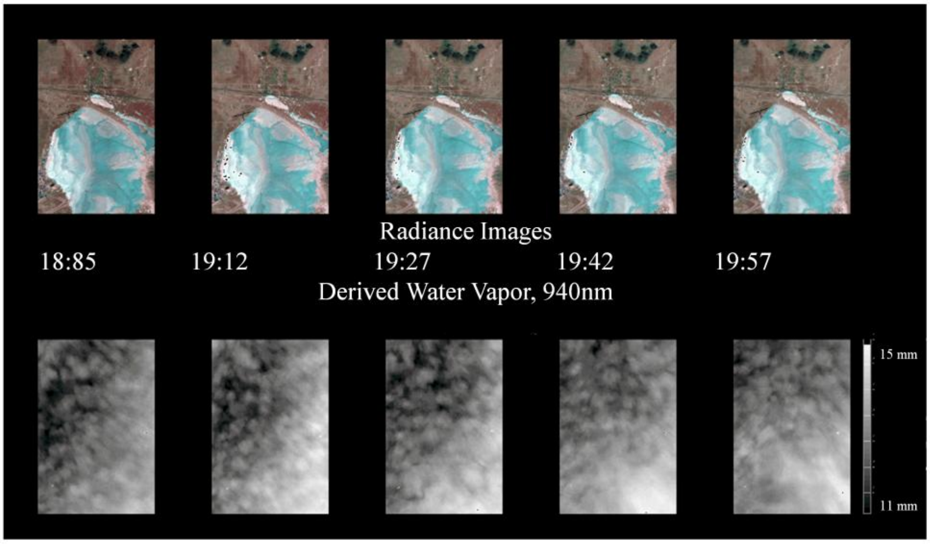

Robert O. Green

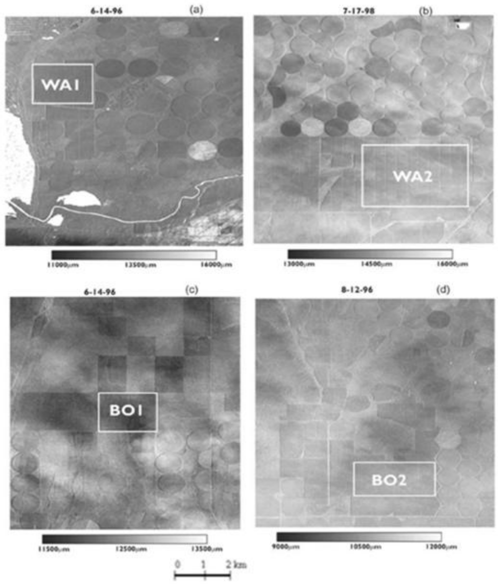

Figure 5. Spatial subset of AVIRIS derived water vapor images of the study sites showing the delineated patches. (a, b, c, d) Column water vapor images corresponding to the false color images shown in Figures 3a, 3b, 3c and 3d, respectively. The dark areas indicate low values of column water vapor while the bright areas indicate high values.

Ogunjemiyo, S., Roberts, D.A., K. Keightley, S.L. Ustin, T. Hinckley, and B. Lamb. 2002. Evaluating the relationship between AVIRIS water vapor and forested land cover. Journal of Geophysical Research-Atmosphere 107 (D23): 4719.

Water vapor
In Fall, Spring
Over Santa Monica
Mts.

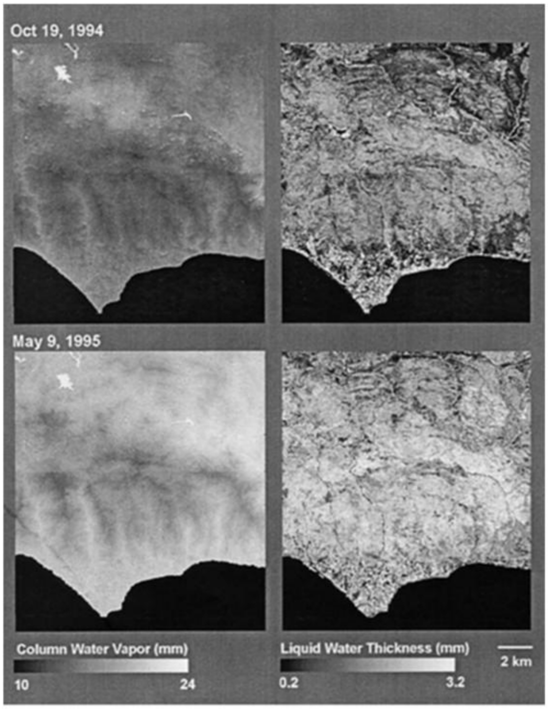

Santa Monica Mountains, CA Measured with AVIRIS

Discriminating Clouds and Snow In Bands Between 1.5 - 2.5 mm

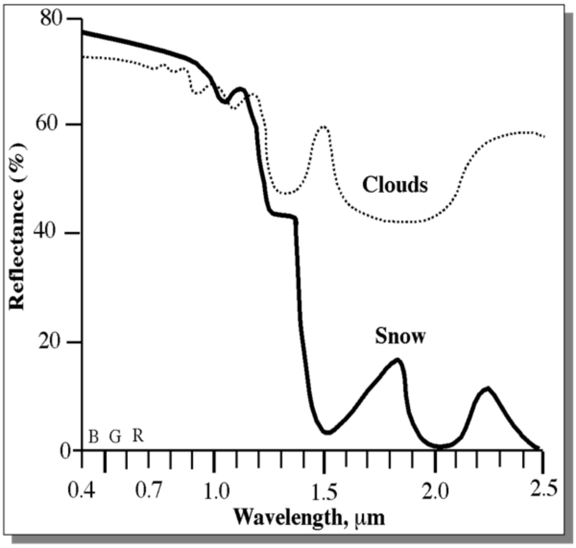

Jensen, 2000

Absorption by Water Vapor, Liquid and Solid Phases in the Solar Reflected Spectrum

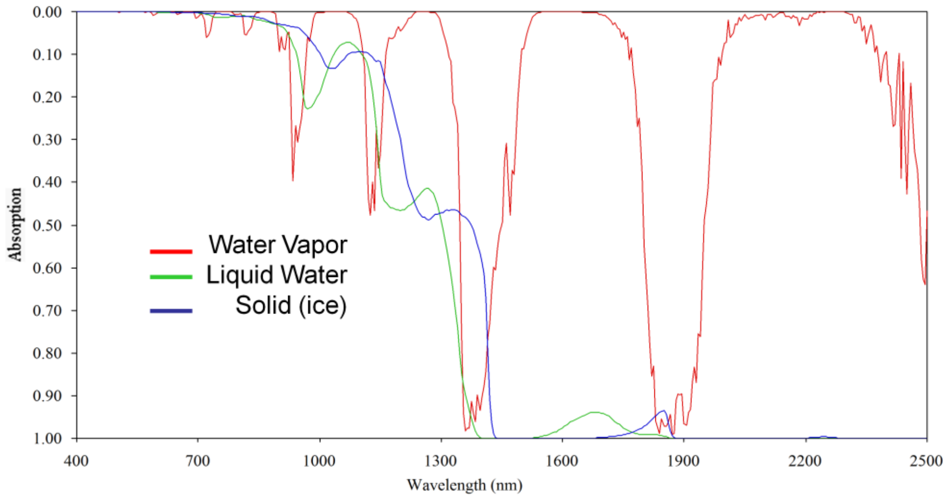

Near 1000 nm absorption spectra for three phases of water overlap but maxima are displaced by wavelength

Robert O. Green

Note that near 1000 nm, that the wavelength of maximum absorption for water vapor is at the shortest wavelength, then liquid water and frozen water at the longest wavelength.

Refectance of Snow

— **Reflectance *increases* as grain size *decreases* - why?**

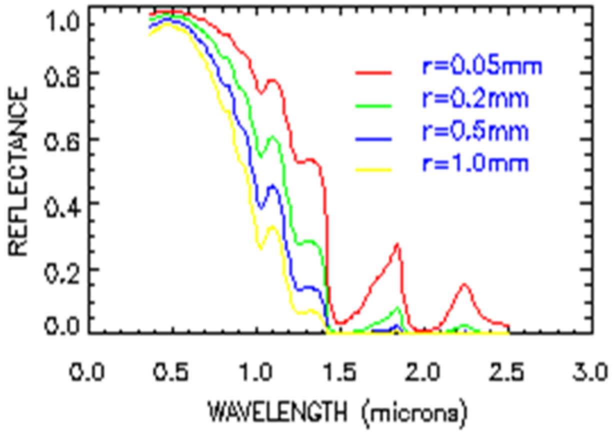

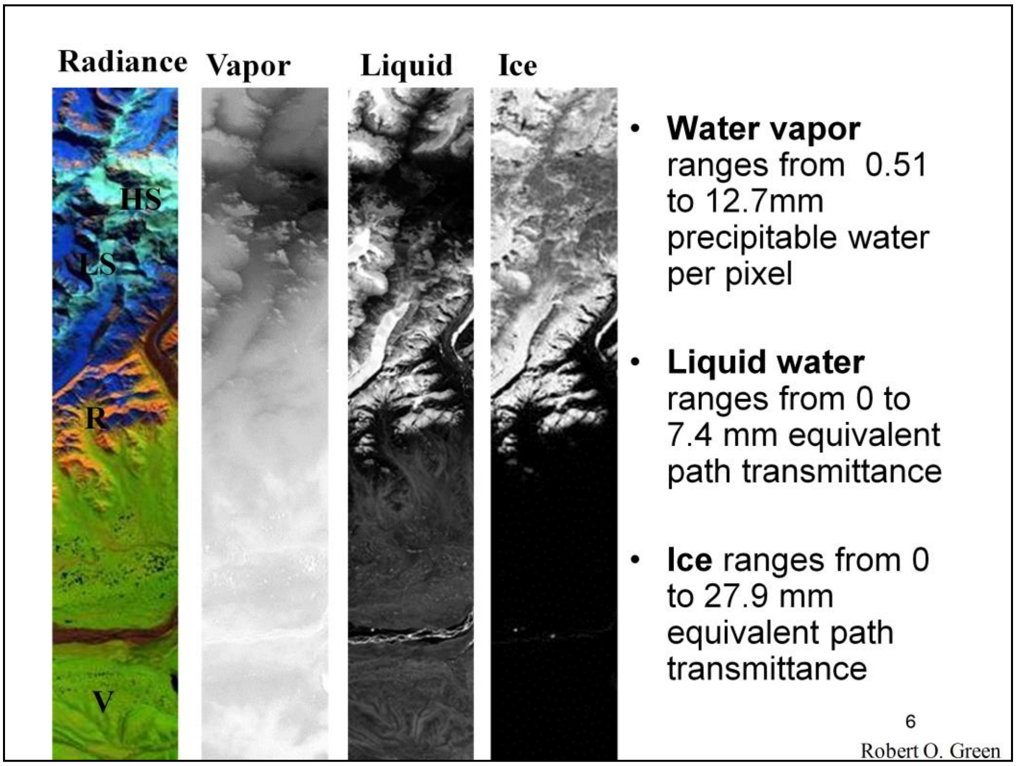

Forward Inversion results for:

V=vegetation
R=rock
LS=low altitude snow
HS= high altitude snow

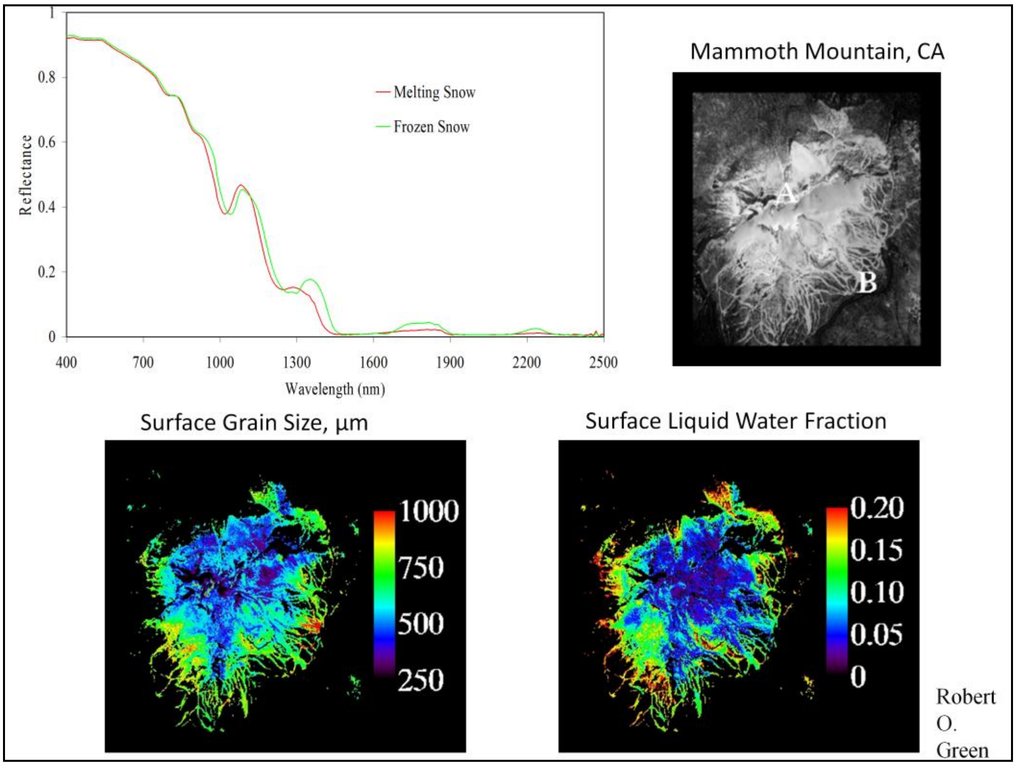

Reflectance
Wavelength (nm)
Melting Snow
Frozen Snow
1
0.8
0.6
0.4
0.2
0
400
700
1000
1300
1600
1900
2200
2500
Mammoth Mountain, CA
A
B
Surface Grain Size, µm
1000
750
500
250
Surface Liquid Water Fraction
0.20
0.15
0.10
0.05
0
Robert O. Green

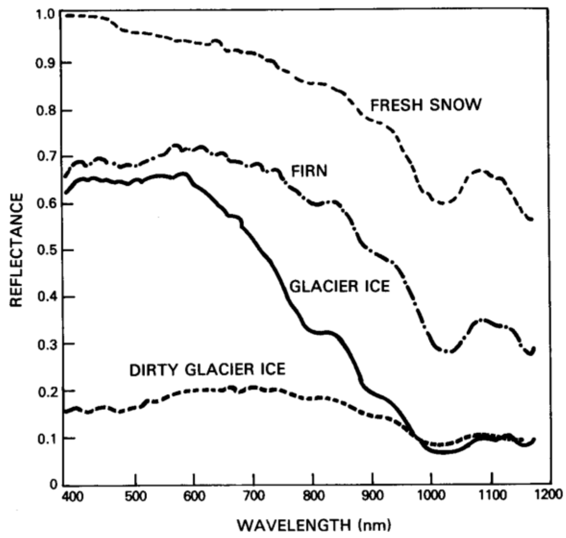

FRESH SNOW
FIRN
GLACIER ICE
DIRTY GLACIER ICE
REFLECTANCE
WAVELENGTH (nm)
1.0
0.9
0.8
0.7
0.6
0.5
0.4
0.3
0.2
0.1
0
400
500
600
700
800
900
1000
1100
1200

Upper Colorado River Basin

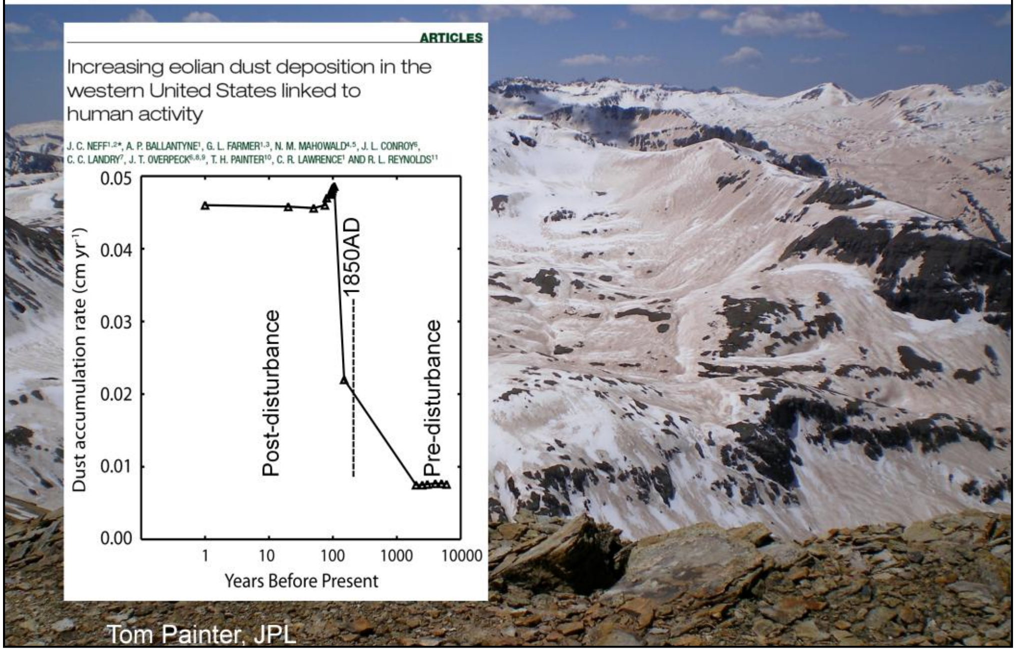


Tien Shan,
Kazakhstan
Tom Painter, JPL

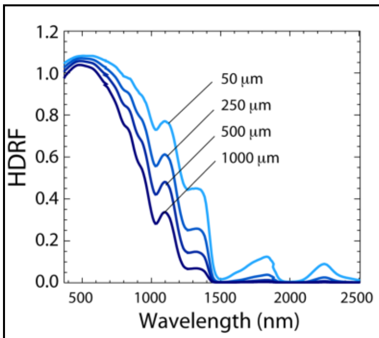

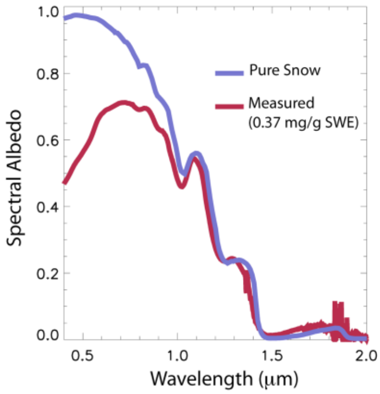

Impact of Dust and Impurities on Snow Reflectance

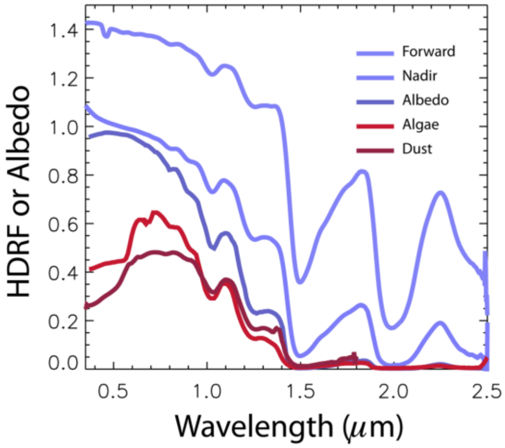

Grain size from integral of ice absorption feature (Clark and Roush 1984; Nolin and Dozier 2000)
- Gives clean snow spectrum against which radiative forcing is determined.

Sources of light contributing to the remotely sensed signal

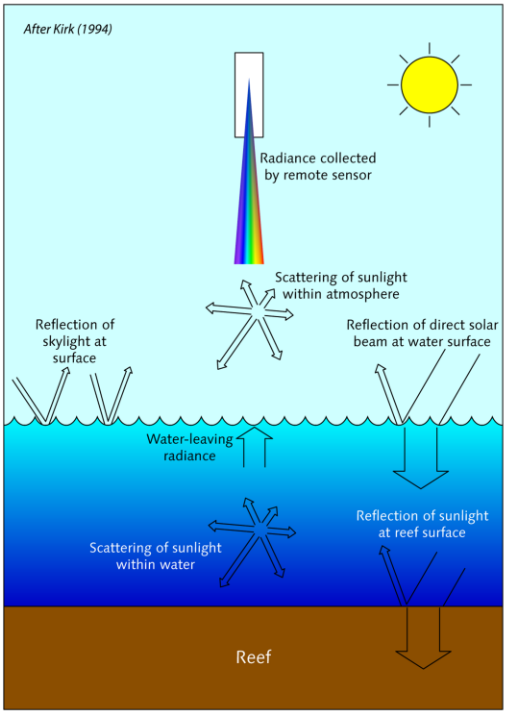

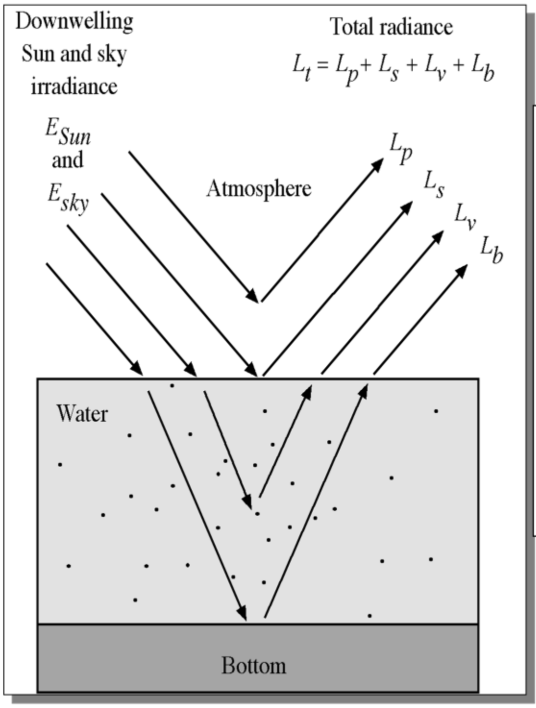

Absorption & Scattering In Water

Total radiance, (L_t) recorded by a remote sensing system over water is a function of the electromagnetic

energy received from:

L_p = atmospheric path radiance

L_s = free-surface layer reflectance

L_v = subsurface volumetric reflectance

L_b = bottom reflectance

How does λ affect this pattern?

Jensen, 2000

Shorter Wavelengtrhs penetrate to deeper depths. Some light can be reflected from bottom. Note refraction between air and water.

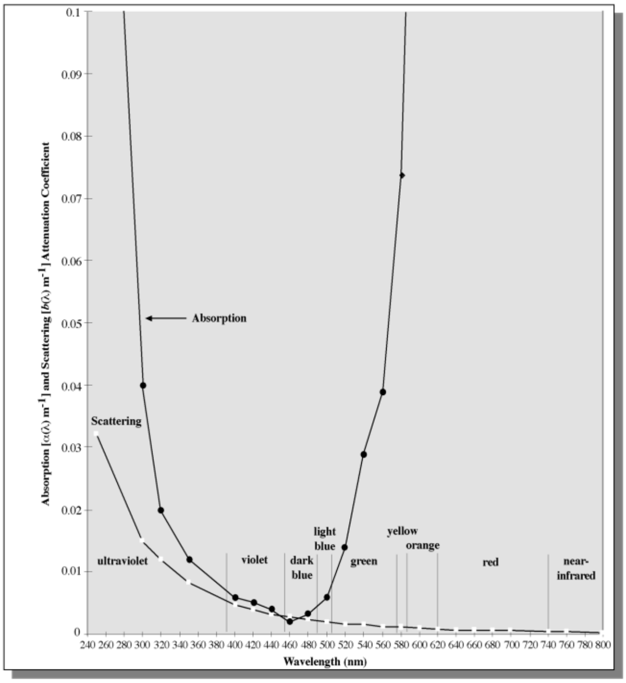

Absorption and Scattering Attenuation in Pure Liquid Water

Scattering in the water column is important in the violet, dark blue, and light blue portions of the spectrum (400 - 500 nm).

Absorption data is truncated in the ultraviolet and in the yellow through NIR regions because the attenuation is so great.

Jensen, 2000

Scattering in the blue is why water appears blue to our eyes.

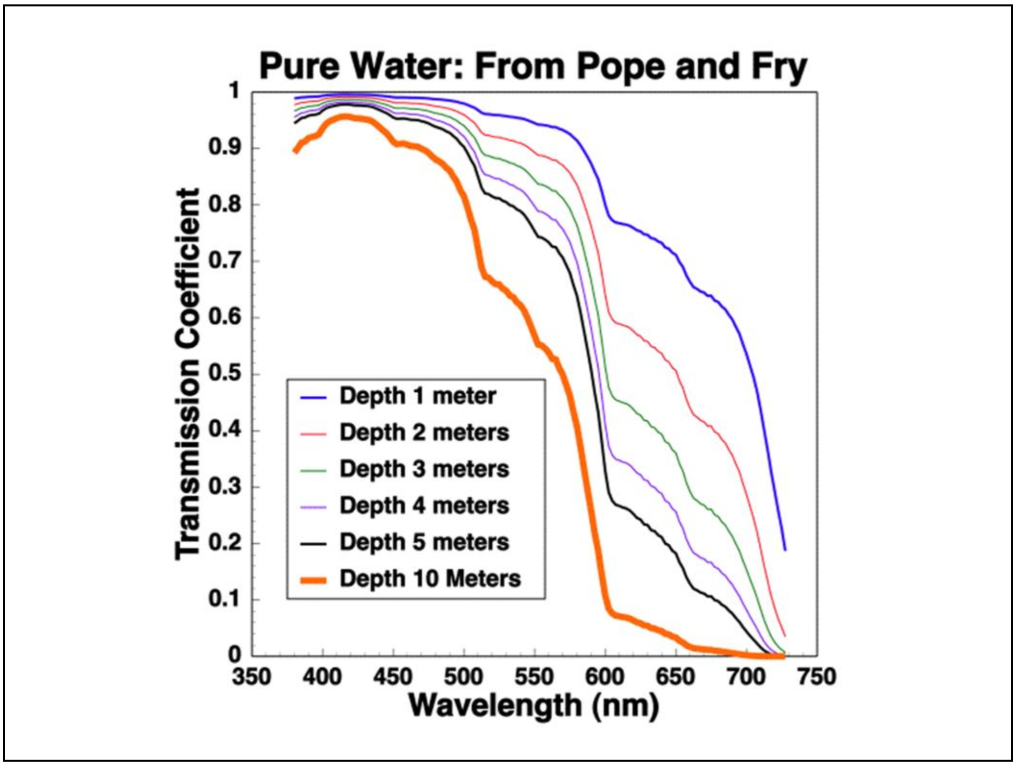

Note that as the depth of water becomes deeper the maximum transmission wavelengths are shifted toward the blue part of the spectrum

Light Penetration Varies with Season: Sediment, Turbidity, Algae, Aquatic Macrophytes

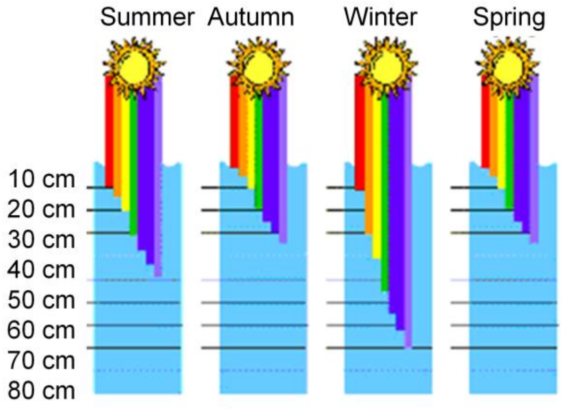

coral reefs over older limestone formations

The islands were named "Dry Tortugas" upon discovery by Ponce de Leon in 1513 -- "tortugas" means turtles in Spanish, and the islands are "dry" as no fresh water is found on them. From the air, the islands present an atoll-like arrangement, however no central volcanic structure is present. The islands are only accessible by boat or seaplane; nevertheless they have been designated the Dry Tortugas National Park, and are visited by hundreds every year. This view highlights three islands in the group; Bush Key, Hospital Key, and Garden Key -- the site of Fort Jefferson. Fort Jefferson is a Civil War era fort, perhaps most notable for being the prison of Dr. Samuel Mudd, who set the broken leg of John Wilkes Booth following Booth's assassination of President Lincoln. The fort itself is currently undergoing extensive restoration to prevent collapse of the hexagonal outer walls (center). The islands stand out due to brown and light tan carbonate sands visible above the Gulf of Mexico water surface. Light blue-green irregular masses in the image surrounding the islands are coral reef tops visible below the water surface.

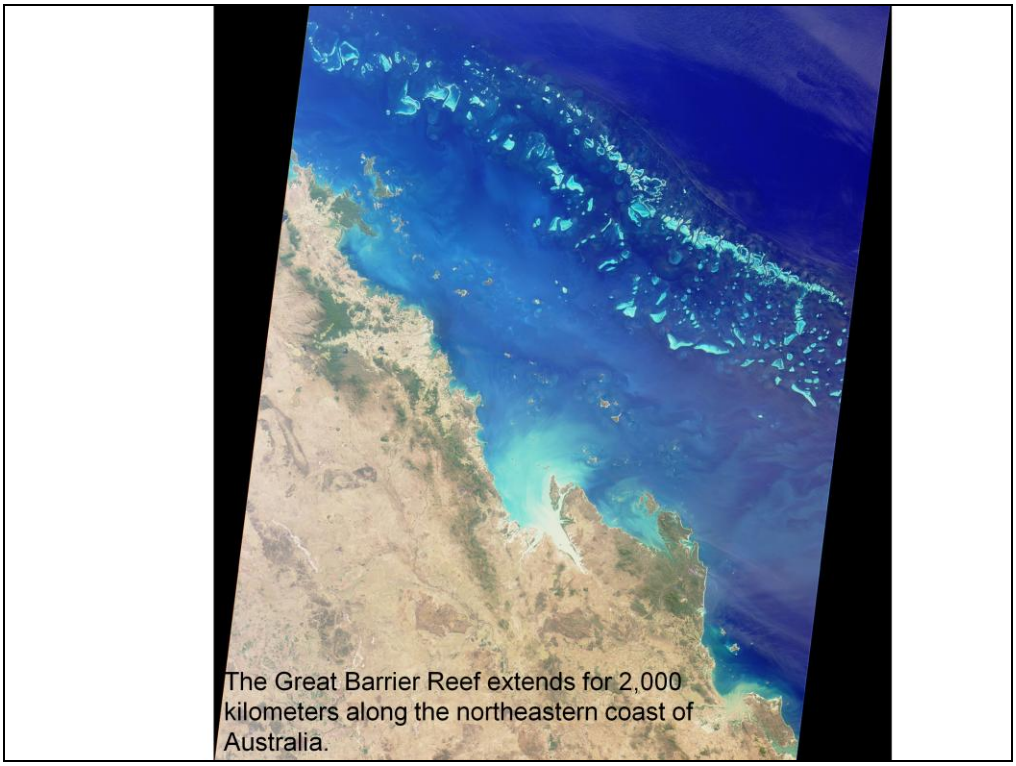

vast maze of reefs, passages, and coral cays (islands that are part of the reef). This nadir true-color image was acquired by the Multi-angle Imaging Spectroradiometer (MISR) instrument on August 26, 2000, and shows part of the southern portion of the reef adjacent to the central Queensland coast. The width of the MISR swath is approximately 380 kilometers, with the reef clearly visible up to approximately 200 kilometers from the coast. It may be difficult to see the myriad details in the browse image, but if you retrieve the higher resolution version, a zoomed display reveals the spectacular structure of the many reefs.

The more northerly coastal area in this image shows the vast extent of sugar cane cultivation, this being the largest sugar producing area in Australia, centered on the city of Mackay. Other industries in the area include coal, cattle, dairying, timber, grain, seafood, and fruit. The large island off the most northerly part of the coast visible in this image is Whitsunday Island, with smaller islands and reefs extending southeast, parallel to the coast. These include some of the better known resort islands such as Hayman, Lindeman, Hamilton, and Brampton Islands.

Further south (in the high-resolution version), just inland of the small semicircular bay near the right of the image, is Rockhampton, the largest city along the central Queensland coast, and the regional center for much of central Queensland. Rockhampton is just north of the Tropic of Capricorn. Its hinterland is a rich pastoral, agricultural, and mining region.

Light Penetration in Water

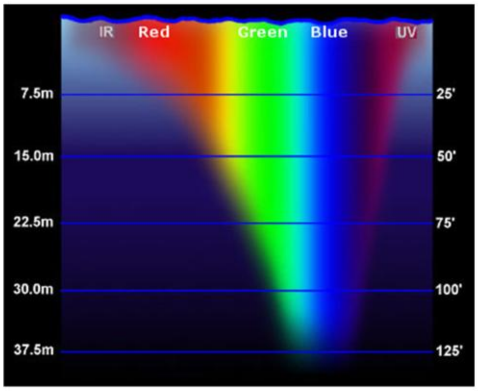

Note Order from long to short wavelengths

Light Penetration in Water

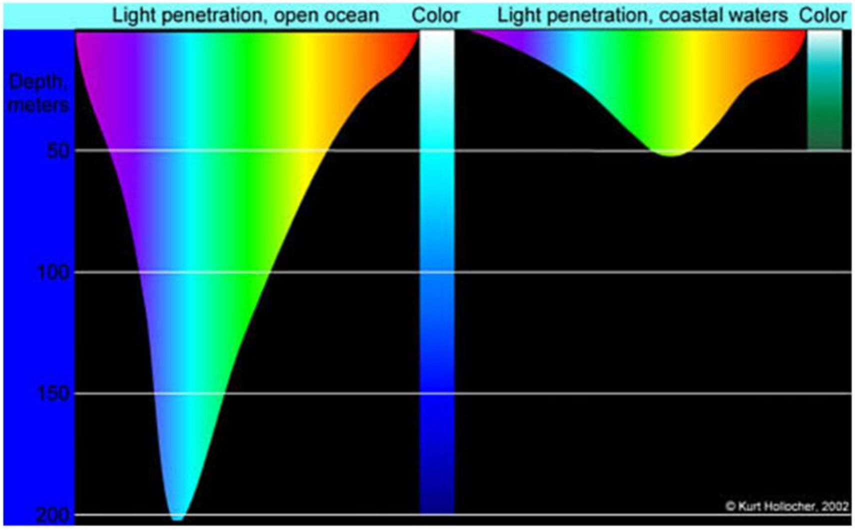

What λ order are these displayed in?

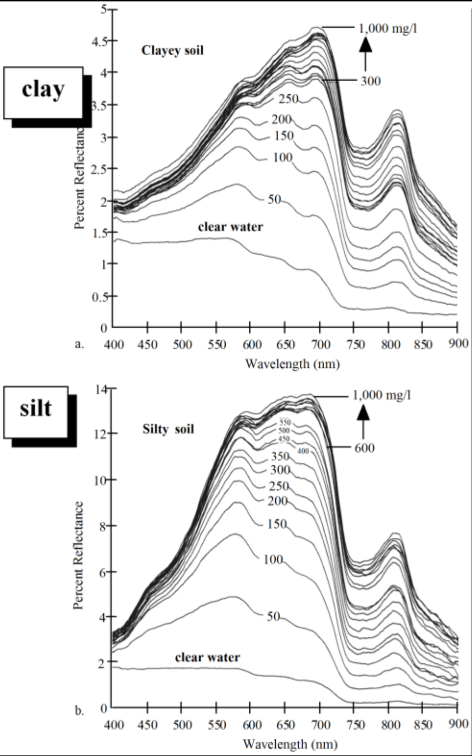

Clear Water with Various Levels of Suspended Clay and Silt Soil Sediment Concentrations

Reflectance peak shifts toward longer wavelengths as more suspended sediment is added

Lodhi et al., 1997;
Jensen, 2000

In situ spectroradiometer Measurements

% reflectance of clear and algae-laden water

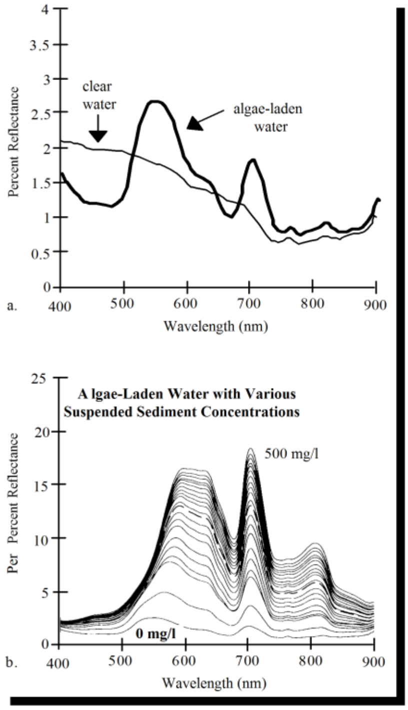

% reflectance of algae-laden water at various suspended sediment concentrations ranging from 0 - 500 mg/l

Han, 1997;
Jensen, 2000

Note strong *chlorophyll a* absorption of blue light between 400 and 500 nm and strong absorption of red light at ~675 nm

Mitigation Options

Subtraction of NIR Reflectance

Example of glint correction using subtraction of NIR reflectance. (Left) Original AVIRIS scene of Kaneohe Bay, Hawaii (f000412t01p03_r08). (Right) The scene after atmosphere and glint correction. Clouds and some sea surface features remain; this is due to automated masking. Overall, glint correction performs quite well.

Source: Bo-Cai Gao

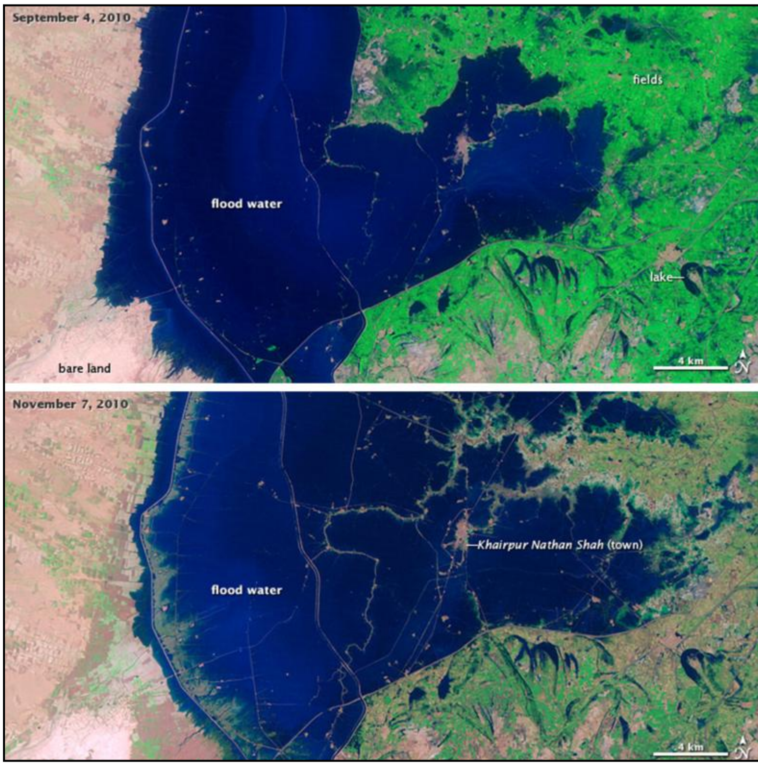

58

Monsoon rains fall on Pakistan every summer, but the summer of 2010 was extraordinary. A combination of factors, including La Niña and a strange jet stream pattern, caused devastating floods. The Indus River rapidly rose, and a dam failure in Sindh Province sent part of the river down an alternate channel. The resulting floodwater lake lingered for months, leaving crops, roads, airports, even entire communities underwater.

The town of Khairpur Nathan Shah was one of many communities affected by the floodwater lake. Normally surrounded by croplands and irrigation infrastructure, the town was instead surrounded by water for months. The Landsat 5 satellite captured these images of the area on September 4, 2010 (top), November 7, 2010 (middle), and January 26, 2011 (bottom). In these false-color images, water appears blue, vegetation appears bright green, and bare land ranges in color from in pink-beige to brick.

The image from September 4 shows water spanning more than 25 kilometers (15 miles) from east to west. Khairpur Nathan Shah pokes above the water, but only partially. By November 7, flood waters appear to have shifted, with some areas are drying out in the west, but a sizable patch newly submerged in the north. By January 26, more areas have emerged from the water, but the region is by no means back to normal.

A complex network of irrigation infrastructure also reappears as the landscape dries out. Once flood water pushed over riverbanks, manmade canals and embankments proved all too effective in holding that water in the wrong places. A new article, Heavy Rains and Dry Lands Don't Mix: Reflections on the 2010 Pakistan Flood, examines the 2010 monsoon and its aftermath. Here is an excerpt.

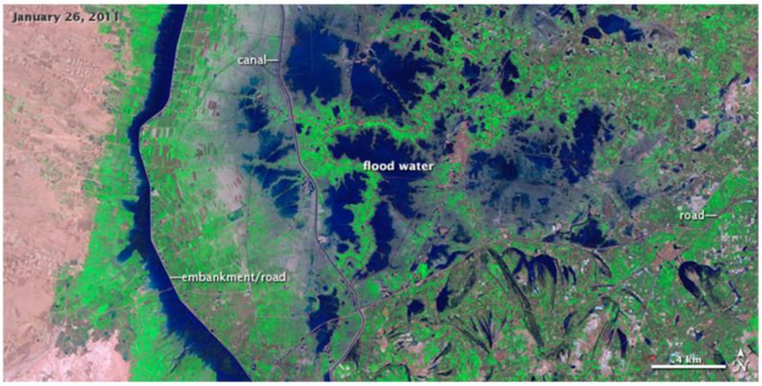

59

Monsoon rains fall on Pakistan every summer, but the summer of 2010 was extraordinary. A combination of factors, including La Niña and a strange jet stream pattern, caused devastating floods. The Indus River rapidly rose, and a dam failure in Sindh Province sent part of the river down an alternate channel. The resulting floodwater lake lingered for months, leaving crops, roads, airports, even entire communities underwater.

The town of Khairpur Nathan Shah was one of many communities affected by the floodwater lake. Normally surrounded by croplands and irrigation infrastructure, the town was instead surrounded by water for months. The Landsat 5 satellite captured these images of the area on September 4, 2010 (top), November 7, 2010 (middle), and January 26, 2011 (bottom). In these false-color images, water appears blue, vegetation appears bright green, and bare land ranges in color from in pink-beige to brick.

The image from September 4 shows water spanning more than 25 kilometers (15 miles) from east to west. Khairpur Nathan Shah pokes above the water, but only partially. By November 7, flood waters appear to have shifted, with some areas are drying out in the west, but a sizable patch newly submerged in the north. By January 26, more areas have emerged from the water, but the region is by no means back to normal.

A complex network of irrigation infrastructure also reappears as the landscape dries out. Once flood water pushed over riverbanks, manmade canals and embankments proved all too effective in holding that water in the wrong places. A new article, Heavy Rains and Dry Lands Don't Mix: Reflections on the 2010 Pakistan Flood, examines the 2010 monsoon and its aftermath. Here is an excerpt.

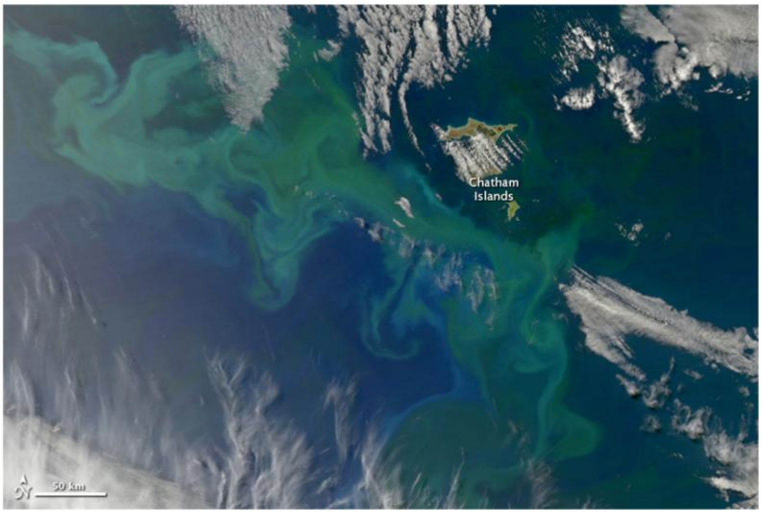

60

The waters around New Zealand's Chatham Islands teem with life. The highly productive waters support massive phytoplankton blooms that sustain valuable stocks of fish. This image, taken by the Moderate Resolution Imaging Spectroradiometer (MODIS) on NASA's Aqua satellite on December 5, 2010, shows the large annual spring-time bloom.

The bloom is an array of colors from deep green to electric blue, and is probably made up of many different types of marine life, primarily phytoplankton. The phytoplankton, plant-like organisms, contribute to making the ocean in this region a carbon sink, a place where the ocean takes in more carbon dioxide than it releases into the atmosphere.

The ocean is productive in this region because the topography of the ocean floor brings two currents together around the Chatham Islands. The islands sit on the Chatham Rise, an underwater plateau that stretches from New Zealand's South Island east to just beyond the Chatham Islands. The water north and south of the plateau is very deep. Cold, nutrient-rich, but iron-poor water from the Antarctic flows south of the Chatham Rise. To the north is mostly warm, nutrient-poor, but iron-rich water from the subtropics.

The two pools of water come together in a current that rides over the plateau, mixing cold water with warm. The mixed water in the current provides both the nutrients and iron fertilizers needed to support large blooms around the Chatham Islands. The current, and therefore, the bloom, is strongest in the spring and fall.

Bright Waters off the Namibian Coast

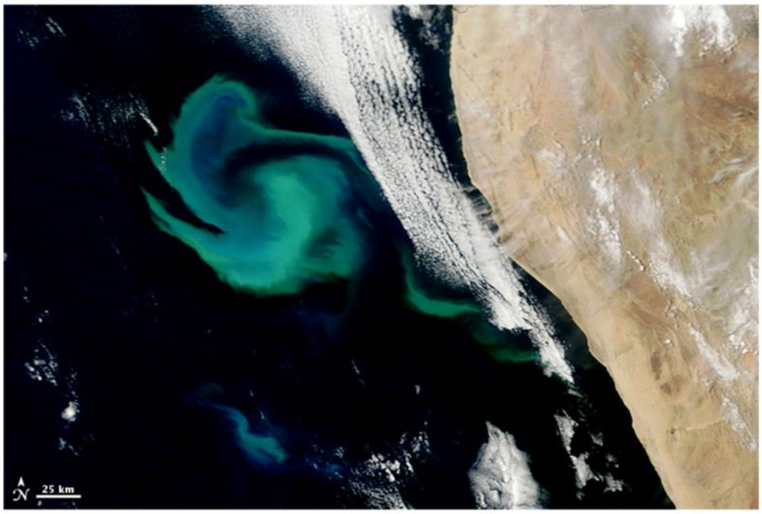

61

Ocean waters glowed peacock green off the northern Namibian coast in late November 2010. The Moderate Resolution Imaging Spectroradiometer (MODIS) on NASA's Terra satellite captured this natural-color image on November 21, 2010.

These bright swirls of green occur along a continental shelf bustling with biological activity. Phytoplankton blooms often occur along coastlines where nutrient-rich waters well up from ocean depths. The light color of this ocean water suggests the calcite plating of coccolithophores.

Farther south along the coast of Namibia, hydrogen sulfide eruptions occur fairly frequently. According to a study published in 2009, ocean currents deliver oxygen-poor water from the north, while the bacteria that break down phytoplankton also consume oxygen, depleting the supply even more. In this oxygen-poor environment, anaerobic bacteria produce hydrogen sulfide gas. When the hydrogen sulfide finally reaches oxygen-rich surface waters, pure sulfur precipitates into the water. The sulfur's yellow mixes with the deep blue ocean to make bright green.

So this swirl of bright green could contain phytoplankton, sulfur, or a combination of the two.

Lecture 5: What you should know about Earth Observing Satellites

1. *Landsat MSS and TM (# bands, approx. λ location, spatial resolution)*
2. SPOT satellites (compared to Landsat *(# bands, approx. λ location, spatial resolution)*
3. Pixel and spatial resolution of Landsat, SPOT
4. Trends: more bands, smaller pixels, more countries, companies flying them, etc.

Lecture 5: What you should know about water

1. Spectral properties of water in all three phases
2. Causes of absorption and scattering in vapor, liquid, ice
3. Effect of particle size on reflectance of ice & water drops in clouds, snow
4. Impact of algae, black carbon, and sediment on ice/snow reflectance
5. Light penetration into water by wavelength
6. Detection of coral, other things in water
7. Effect of specular reflection on water (sunglint)